



Synthesis and biological evaluation of 1-(benzofuran-3-yl)-4-(3,4,5-trimethoxyphenyl)-1*H*-1,2,3-triazole derivatives as tubulin polymerization inhibitors

Zhi-Yuan Qi^{a,1}, Shu-Yi Hao^{a,1}, Heng-Zhi Tian^a, Hong-Li Bian^a, Ling Hui^b, Shi-Wu Chen^{a,*}

^a School of Pharmacy, Lanzhou University, Lanzhou 730000, China

^b Experimental Center of Medicine, General Hospital of Lanzhou Military Command, Lanzhou 730050, China

ARTICLE INFO

Keywords:

Microtubule
Tubulin polymerization
Benzo[b]furan
1,2,3-Triazole
Antitumor

ABSTRACT

The key functions of microtubules and the mitotic spindle in cell division make them attractive targets for cancer therapy. In this study, a series of 1-(benzofuran-3-yl)-4-(3,4,5-trimethoxyphenyl)-1*H*-1,2,3-triazole derivatives was synthesized, and their antiproliferative activities against HCT116, HeLa, HepG2, and A549 cells were evaluated. 6-Methoxy-*N*-phenyl-3-(4-(3,4,5-trimethoxyphenyl)-1*H*-1,2,3-triazol-1-yl)benzofuran-2-carboxamide (**17g**) exhibited the strongest antiproliferative activities, with IC₅₀ values ranging from 0.57 to 5.7 μM. Mechanistic studies showed that **17g** inhibited tubulin polymerization, leading to the disruption of mitotic spindle formation, cell cycle arrest in the G2/M phase, and apoptosis of A549 cells. A docking study indicated that **17g** was a good molecular fit at the colchicine binding site of tubulin. These results showed that **17g** is a potential anticancer compound that is worthy of further development as a tubulin polymerization inhibitor.

1. Introduction

Microtubules are long, hollow tubular structures that predominantly consist of α , β -tubulin dimers [1]. They are involved in many structural functions, including cell division, signaling, motility, cell maintenance, and intracellular vesicle transport, and have become attractive targets for novel antimetabolic drugs for cancer therapy [2]. The binding sites of microtubule-targeting drugs include the colchicine, vinca, and taxane sites. In general, compounds that bind to the colchicine and vinca sites are tubulin polymerization inhibitors, whereas those that bind to the taxane site are polymerization stabilizers [3,4]. Inhibitors that bind to the colchicine site have drawn the most attention, because these compounds have the potential to overcome ABC-transporter-mediated drug resistance and vascular disrupting properties [5–7].

Colchicine (**1**, Fig. 1) was the first drug known to function as a tubulin polymerization inhibitor [8]. However, the therapeutic value of its anticancer activity is restricted by its toxicity and low therapeutic index [9]. Combretastatin A-4 (CA-4, **2**), another inhibitor that binds at the colchicine site, was first isolated from the bark of *Combretum caffrum*, and displays potent cytotoxicity against a wide range of cancer cell lines. However, its poor water solubility and bioavailability hindered its development into an antitumor drug [10]. To overcome these

shortcomings, its water-soluble ester, CA-4P (**3**), was prepared and entered clinical trials for the treatment of platinum-resistant ovarian cancer. Unfortunately, that study was terminated in 2017 owing to a lack of efficacy for improving progression-free survival (PFS), combined with an unfavorable objective response rate (ORR) [11].

Structure–activity relationship studies of CA-4 derivatives have indicated that the 3,4,5-trimethoxybenzene (A ring) is critical for bioactivity [12–16] and that the 3-hydroxy-4-methoxybenzene (B ring) might be replaced with various heterocycles [17,18]. Furthermore, there is evidence to suggest that maintaining a *cis*-configuration between the A and B rings is important for optimal bioactivity [17,18]. Flynn and coworkers reported that BNC105 (**4**), which contains a benzo [b]furan as the B ring, exhibited excellent antiproliferative activity against MCF-7 cells (IC₅₀ = 0.002 μM) and tubulin polymerization inhibitory activity (IC₅₀ = 3.0 μM) [19]. Furthermore, its water-soluble phosphate, BNC105P (**5**), exhibited potent effects on mesothelioma, and ovarian and renal cancers, in clinical trials [20]. Odlo et al. also reported that the vinyl group in CA-4 can be substituted with 1,2,3-triazolyl to maintain the *cis*-configuration of the A and B rings. The resulting compound (**6**) exhibited strong antiproliferative activity against K562 cells, with an IC₅₀ value of 3.20 μM [21].

Triazoles are five-membered rings with numerous applications as

* Corresponding author.

E-mail address: chenshw@lzu.edu.cn (S.-W. Chen).

¹ These authors made equal contributions to this work.

<https://doi.org/10.1016/j.bioorg.2019.103392>

Received 22 June 2019; Received in revised form 4 September 2019; Accepted 21 October 2019

0045-2068/ © 2019 Elsevier Inc. All rights reserved.

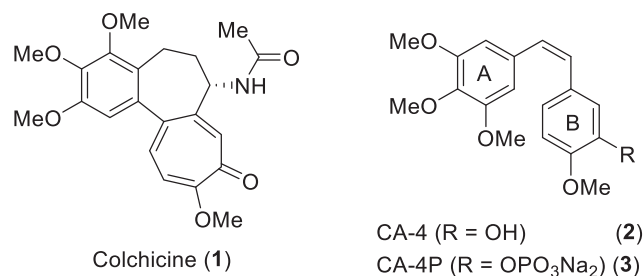


Fig. 1. Chemical structures of colchicine (1), CA-4 (2) and CA-4P (3).

linkers in medicinal chemistry [22,23]. To discover novel inhibitors based on CA-4 with strong antitumor activities, we designed a series of 1-(benzofuran-3-yl)-4-(3,4,5-trimethoxyphenyl)-1H-1,2,3-triazole derivatives that are hybrids of compounds 4 and 6. These hybrid compounds contain both benzo[*b*]furan and 1,2,3-triazolyl moieties (Fig. 2). Herein, we report the synthesis and antiproliferative activities of a set of novel target compounds. Furthermore, we report the biological activity of representative compound 17g, including its effect on *in vitro* tubulin polymerization, intracellular microtubule networks, cell cycle arrest, cell apoptosis, and the mitochondrial membrane potential (MMP) of A549 cells. Furthermore, molecular modeling studies of the colchicine binding site of tubulin were performed with 17g.

2. Results and discussion

2.1. Chemistry

The synthetic routes to the target compounds are outlined in Schemes 1 and 2. Initially, we synthesized intermediate 5-ethynyl-1,2,3-trimethoxybenzene (9) from 3,4,5-trimethoxybenzaldehyde (7) as the starting material using the Corey–Fuchs reaction [24]. Specifically, 5-(2,2-dibromovinyl)-1,2,3-trimethoxybenzene (8) was obtained from the reaction of 7 with PPh₃ and CBr₄. Compound 8 was then treated with *n*-BuLi at –78 °C to yield alkyne derivative 9 [25].

Tandem one-pot cyclization of 2-hydroxy benzonitrile derivatives 10a,b with ethyl bromoacetate and K₂CO₃ in DMF afforded 2-ethoxycarbonyl-3-amino benzo[*b*]furan derivatives 11a,b [17]. Next, the azidation of 11a,b was accomplished in the presence of NaNO₂ and NaN₃ in acetic acid to obtain 12a,b [26]. The ester group of 12a,b was

hydrolyzed to give 13a,b, and the resulting carboxylic acids were esterified with isopropanol using 1-(3-dimethylaminopropyl)-3-ethylcarbodiimide hydrochloride (EDC·HCl) and *N,N*-dimethylaminopyridine (DMAP) catalysis to give 14b and 15b [27]. Amidation of 13a,b with various amines using EDC·HCl and 1-hydroxybenzyltriazole hydrate (HOBT) catalysis yielded 14c–i and 15c–i [28]. Finally, the 18 target compounds were synthesized by click reactions between 12a, 14b–i or 12b, 15b–i, and 9 [21,29].

2.2. Biological profiling

2.2.1. Antiproliferative activities of compounds 16a–i, 17a–i

Novel compounds 16a–i and 17a–i were evaluated for antiproliferative activity against four human cancer cell lines (HCT116 colon cancer, HepG2 hepatic carcinoma, HeLa human epithelial cervical cancer, and A549 non-small-cell lung cancer) using the MTT assay with CA-4 as a reference drug [30]. The IC₅₀ values of the compounds (concentrations corresponding to 50% inhibition of cell growth) are summarized in Table 1.

Compounds 16a–i were unsubstituted at the 6-position, whereas their analogues 17a–i were the corresponding 6-methoxy derivatives. This allowed us to investigate the effect of the 6-methoxy group on antiproliferative activity. As shown in Table 1, the IC₅₀ values of 17a–i were lower than those of the corresponding unsubstituted compounds 16a–i (for example, 17a vs. 16a, 17b vs. 16b), indicating that the 6-methoxy group was beneficial for antiproliferative activity. Compounds 16a,b and 17a,b, possessing either ethoxycarbonyl or isopropoxycarbonyl groups at the 2-position, showed poor antiproliferative activities, while 2-amido-substituted compounds 16c–i and 17c–i showed higher activities. Among them, 6-methoxy-*N*-phenyl-3-(4-(3,4,5-trimethoxyphenyl)-1H-1,2,3-triazole-1-benzofuran-2-carboxamide (17g) exhibited the highest activity, with IC₅₀ values against HCT-116, HeLa, HepG2, and A549 cells of 0.87 ± 0.79, 0.73 ± 0.67, 5.74 ± 1.21 and, 0.57 ± 0.31 μM, respectively. Furthermore, the compounds substituted with cyclopropylamine, piperidine, and morpholine showed lower cytotoxic activities than those substituted with aniline (16h,i vs. 16g, 17h,i vs. 17g). Furthermore, compounds 16c, 16g and 17g were also evaluated for their toxicity toward normal human liver cells HL-7702, the results evaluated that 16g and 17g showed lower toxicity than that of CA-4 (Table 1). Considered compound 17g showed the most potent inhibitory activities against tumor cells and less toxicity toward normal cells, following compound 17g

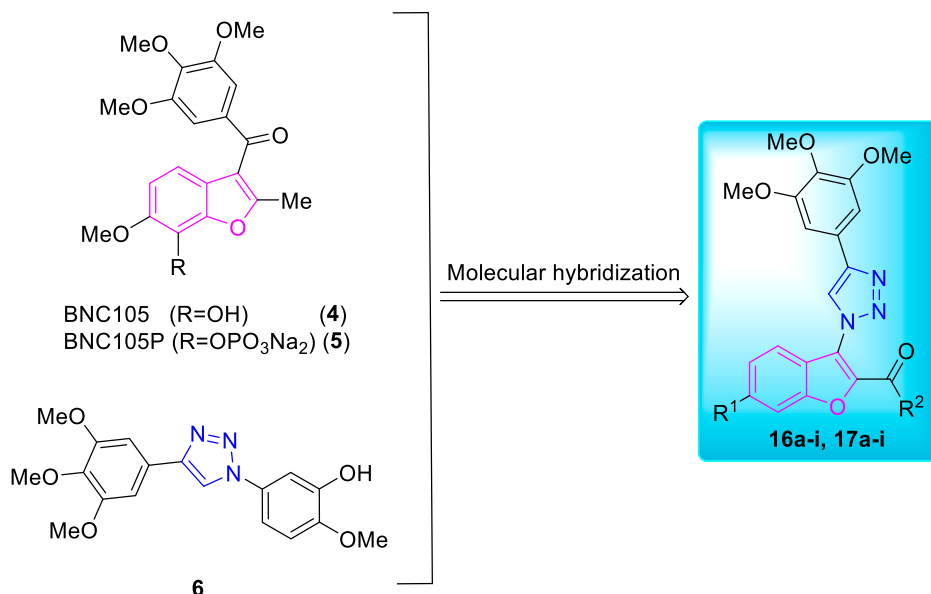
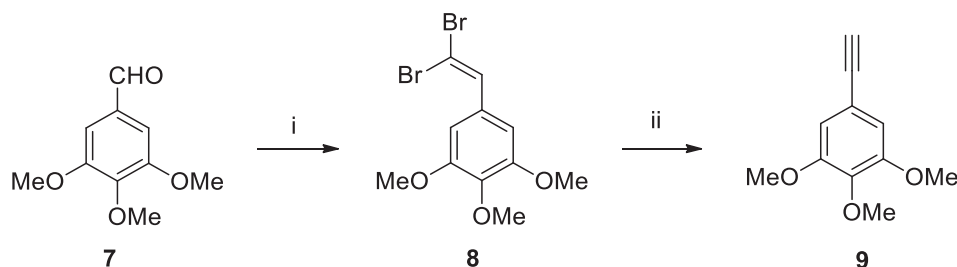


Fig. 2. Design of target compounds 16a–i and 17a–i.



Scheme 1. Reagents and conditions: (i) CBr_4 , PPh_3 , DCM , 0°C , 2 h; (ii) $n\text{-BuLi}$, dry THF , -78°C , 5 h.

was selected to further study its action mechanism in A549 cells.

2.2.2. *In vitro* tubulin polymerization inhibition activity of compound 17g

Mechanistic research has shown that the potent anticancer activity of CA-4 is based on its inhibition of tubulin polymerization [10]. To identify the target of compound 17g, we measured the *in vitro* tubulin polymerization inhibition activity of 17g using the method originally described by Shelanski et al. [31]. As shown in Fig. 3A and 3B, the absorbance intensity of purified and unpolymerized tubulin increased with time, indicating that tubulin polymerization had occurred. After tubulin was incubated with 17g at various concentrations (ranging from 0.6 to 20.0 μM), the change in absorbance intensity was reduced compared with the control (Fig. 3A). This indicated that 17g inhibited tubulin polymerization in a dose-dependent manner. The IC_{50} value of polymerization inhibition was determined as $4.1 \pm 0.1 \mu\text{M}$ (Fig. 3A), which was only slightly higher than that of CA-4 ($1.0 \pm 0.1 \mu\text{M}$, Fig. 3B). Therefore, compound 17g was a potent inhibitor of tubulin polymerization.

2.2.3. Effect of 17g on microtubule organization in A549 cells

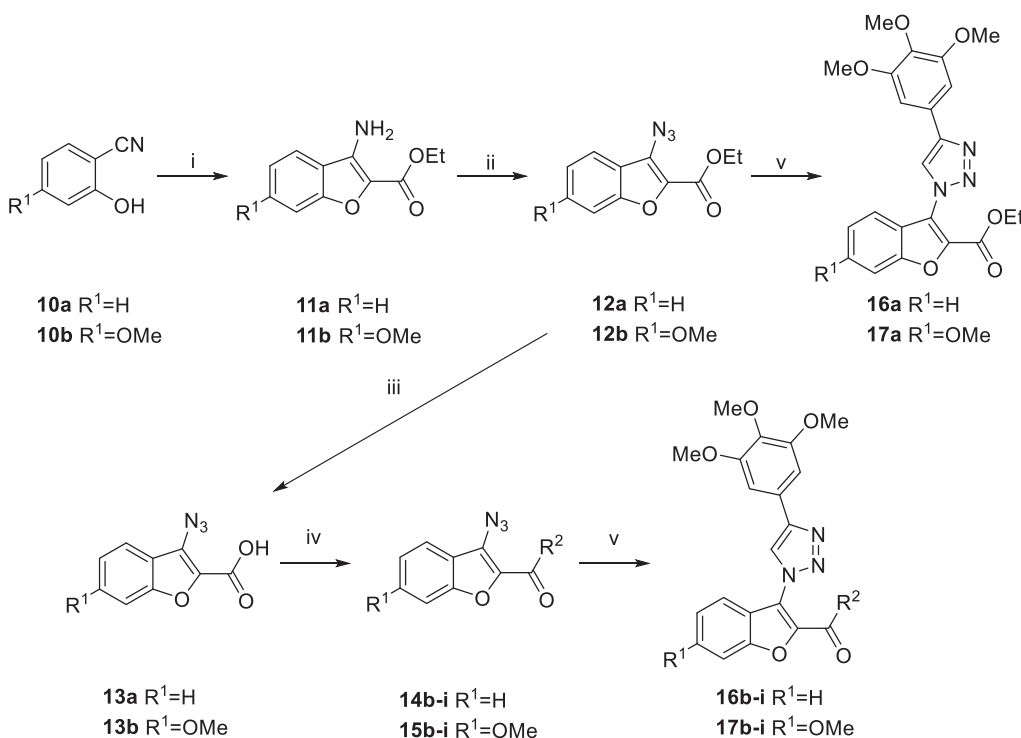
The tubulin–microtubule system plays a vital role in the maintenance of cell shape and basic cellular functions. The inhibition of tubulin polymerization leads to the destruction of microtubule tissue and the cytoskeleton [2]. An immunofluorescence assay was performed to determine whether 17g disrupted the microtubule organization in living A549 cells [32]. As shown in Fig. 4, the microtubule networks in

the control group exhibited a normal arrangement, with slim and fibrous microtubules wrapped around the cell nucleus. However, when the cells were treated with 17g at concentrations of 1.25 and 2.50 μM , the microtubule network tissue was destroyed and shrank to the nucleus. When the compound concentration was increased to 5.00 μM , the spindle formation adopted distinct abnormalities and was heavily disrupted. Furthermore, the microtubule spindles shrank around the center of the cells, and a number of dotted disorder formations were observed. This effect was analogous to that of CA-4 at 5.00 μM . Therefore, 17g disrupted the microtubule organization in A549 cells, which could potentially lead to cell cycle disorder [4].

2.2.4. Effect of 17g on the A549 cell cycle in the G2/M phase

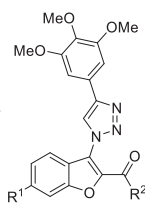
Microtubules play an important role in the movement of chromosomes during cell division. As most tubulin destabilizing agents disrupt the regulated cell cycle distribution [33], flow cytometry analysis was performed to determine the effect of 17g on the cell cycle. As shown in Fig. 5A and 5B, when A549 cells were treated with 17g at 0.5 μM for 24 h, 60% of the cells were arrested in the G2/M phase. This effect was intensified when the concentration of 17g was increased to 2.5 μM , with the percentage of cells at the G2/M phase increasing to 63%. For CA-4, the proportion of cells in the G2/M phase increased from 6% in the control to 69% at 2.5 μM . These results verified that 17g induced cell cycle arrest in the G2/M phase.

Furthermore, cyclin B1, Cdc25C, and Cdc2 are known to be key regulators in cell cycle progression [34,35]. Therefore, the effect of 17g



Scheme 2. Reagents and conditions: (i) ethyl bromoacetate, K_2CO_3 , DMF , 60°C for 8 h, then 140°C for 8 h; (ii) NaNO_2 , NaN_3 , 10:1 acetic acid/ H_2O , 0°C , 2.5 h; (iii) 6 N NaOH , THF and H_2O , rt, 2d; (iv) isopropanol (for 14b and 15b), $\text{EDC}\cdot\text{HCl}$, DMAP , 24 h; or various amines (for 14c-i and 15c-i), $\text{EDC}\cdot\text{HCl}$, HOBT , DCM , rt, overnight; (v) 9, $\text{CuSO}_4\cdot 5\text{H}_2\text{O}$, sodium ascorbate, 1:1 $t\text{-BuOH}/\text{H}_2\text{O}$, rt, overnight.

Table 1

Antiproliferative activities of compounds **16a-i** and **17a-i**.

Compd	R ¹	R ²	IC ₅₀ (μM) ^{a,b}				
			HCT-116	HeLa	HepG2	A549	HL-7702
16a	H	OCH ₂ CH ₃	> 100	> 100	30.97 ± 6.24	> 100	–
16b	H	OCH(CH ₃) ₂	41.71 ± 8.94	59.30 ± 5.15	58.00 ± 9.48	> 100	–
16c	H	HN(CH ₂ CH ₂) ₂	16.43 ± 4.19	6.84 ± 0.34	2.92 ± 0.22	9.29 ± 3.66	18.34 ± 6.04
16d	H	HN(CH ₂) ₂	> 100	> 100	> 100	> 100	–
16e	H	HN(CH ₂) ₃	6.07 ± 0.38	43.37 ± 7.55	36.82 ± 5.43	22.52 ± 2.65	–
16f	H	HN(CH ₂) ₄	8.59 ± 5.47	24.99 ± 7.71	51.12 ± 9.75	94.74 ± 8.93	–
16g	H	HN(CH ₂) ₅	1.02 ± 0.31	1.83 ± 0.52	8.34 ± 2.53	0.83 ± 0.34	36.87 ± 1.26
16h	H	HN(CH ₂) ₆	73.52 ± 17.17	> 100	65.23 ± 5.42	73.99 ± 7.86	–
16i	H	HN(CH ₂) ₇	> 100	> 100	64.85 ± 2.98	> 100	–
17a	OMe	OCH ₂ CH ₃	36.64 ± 7.30	> 100	11.57 ± 3.59	> 100	–
17b	OMe	OCH(CH ₃) ₂	40.21 ± 4.23	29.48 ± 0.67	14.79 ± 5.02	50.41 ± 7.88	–
17c	OMe	HN(CH ₂ CH ₂) ₂	52.46 ± 8.74	2.84 ± 0.95	6.29 ± 2.93	> 100	–
17d	OMe	HN(CH ₂) ₂	> 100	78.38 ± 7.48	> 100	> 100	–
17e	OMe	HN(CH ₂) ₃	1.27 ± 0.38	7.66 ± 1.26	20.26 ± 9.05	18.95 ± 3.17	–
17f	OMe	HN(CH ₂) ₄	5.56 ± 1.76	29.99 ± 5.59	41.65 ± 6.01	> 100	–
17g	OMe	HN(CH ₂) ₅	0.87 ± 0.79	0.73 ± 0.67	5.74 ± 1.21	0.57 ± 0.31	34.33 ± 4.60
17h	OMe	HN(CH ₂) ₆	47.79 ± 7.56	> 100	6.83 ± 3.21	38.79 ± 16.90	–
17i	OMe	HN(CH ₂) ₇	80.08 ± 0.86	49.75 ± 11.74	10.92 ± 4.65	37.85 ± 6.96	–
CA-4	–	–	0.08 ± 0.03	0.17 ± 0.01	0.15 ± 0.02	0.04 ± 0.01	16.60 ± 4.53

^a IC₅₀ values are presented as the means ± SD of triplicate experiments.

^b Drug treatment for 72 h.

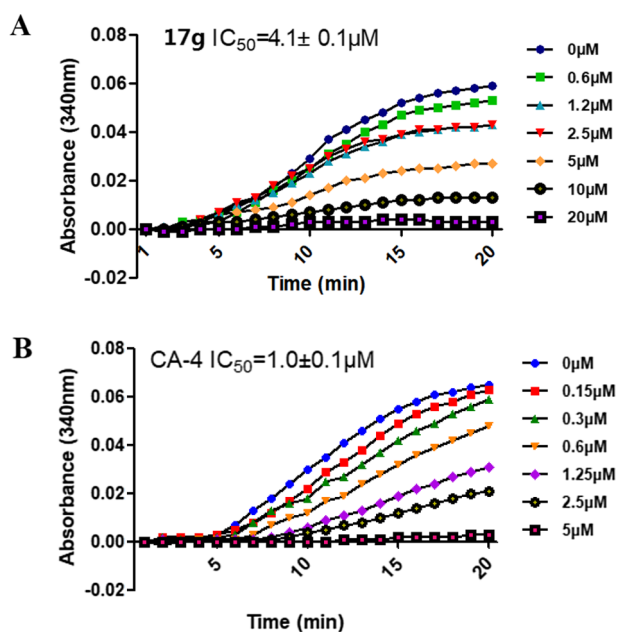


Fig. 3. Tubulin polymerization inhibitory activity of **17g** (A) and CA-4 (B). Purified tubulin protein at 10 μM was incubated at 37 °C in the absence or presence of **17g** and CA-4 at the indicated concentrations.

on the expression of these proteins was investigated by Western blot analysis. As shown in Fig. 5C, after A549 cells were treated with **17g** at concentrations of 0.125, 0.25, and 0.5 μM for 12 h, the expression of cyclin B1, Cdc25C, and Cdc2 proteins decreased in a dose-dependent manner. These results indicated that **17g** can block A549 cells at the G2/M phase, analogous to CA-4, by regulating the expression of cycle-related proteins.

2.2.5. Effect of **17g** on A549 cells apoptosis

Mitotic arrest of tumor cells by tubulin destabilizing agents is generally associated with cellular apoptosis [36,37]. Therefore, the apoptotic effect of **17g** on A549 cells was measured, using CA-4 as a reference compound. As shown in Fig. 6A, after A549 cells were treated with **17g** at concentrations of 0.1 and 2.5 μM for 12 h, the percentage of apoptotic cells was determined to be 5.68% and 8.72%, respectively. These percentages were greater than that under the control conditions, which afforded a 3.34% apoptosis rate, indicating that **17g** induced A549 cell apoptosis. However, the 8.72% apoptosis rate caused by **17g** at 2.5 μM was significantly lower than that of CA-4 at an equivalent concentration (30.71%). This was consistent with the lower antiproliferative activities of **17g** compared with those of CA-4.

Bcl-2 and Bcl-xl are important antiapoptotic proteins, while Bax is an important proapoptosis protein [38]. Therefore, the effect of **17g** on the expression of Bcl-2, Bcl-xl, and Bax proteins was investigated. As shown in Fig. 6B and 6C, when A549 cells were treated with **17g** at different concentrations (0.125, 0.25, and 0.5 μM) for 6 h, the

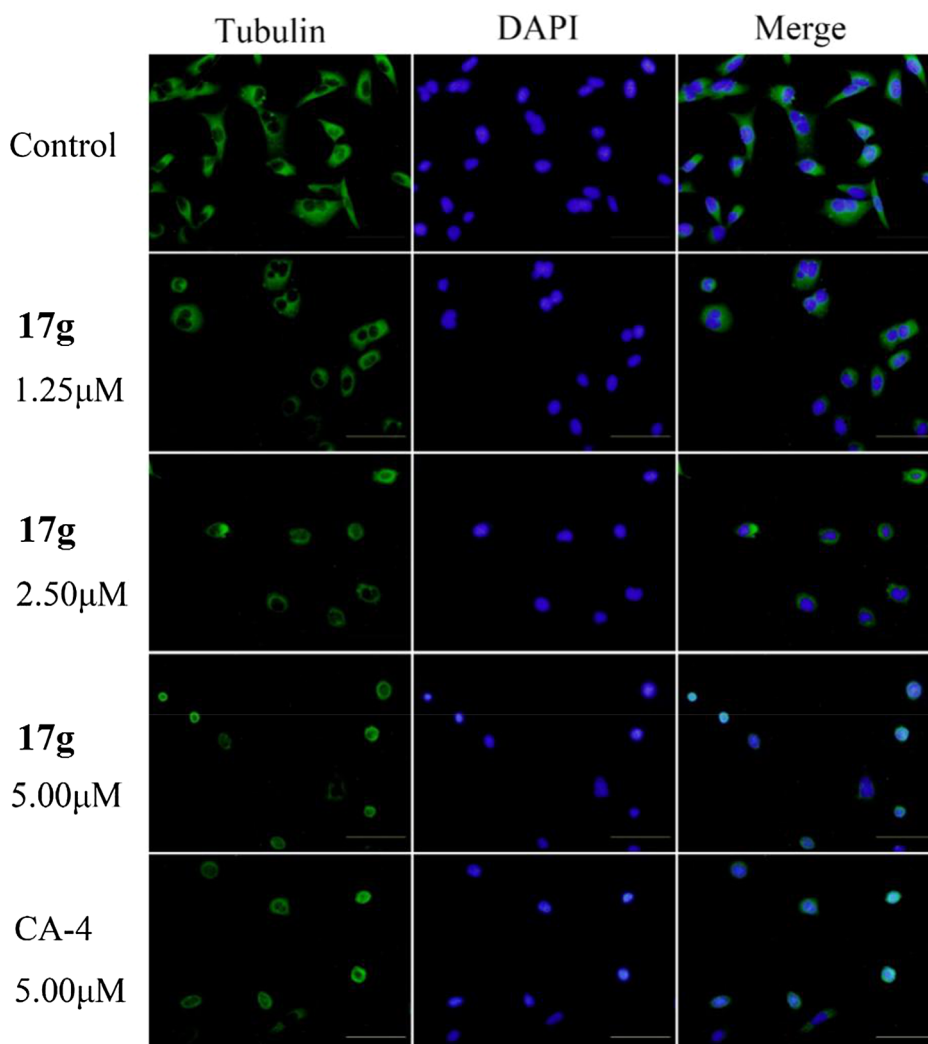


Fig. 4. Effect of compound **17g** on organization of the cellular microtubule network in A549 cells. A549 cells were plated in confocal dishes and incubated with **17g** or CA-4 at the indicated concentrations for 6 h, followed by direct microscopy, with representative immunofluorescence shown. Scale bar: 10 μm .

expression level of antiapoptotic proteins (Bcl-2, Bcl-xl) was down-regulated significantly. However, **17g** had no significant effect on the expression level of proapoptosis protein Bax. These results demonstrated that **17g**, similar to CA-4, can downregulate the expression of antiapoptotic proteins, leading to cell apoptosis.

2.2.6. Effect of **17g** on the mitochondrial membrane potential (MMP)

Previous studies have indicated that mitochondria play a vital role in the progression of apoptosis [39]. Decreased MMP ($\Delta\Psi\text{m}$) has been implicated as an early event in apoptotic cells. Therefore, we measured the effect of **17g** on MMP changes in A549 cells. As shown in Fig. 7, after A549 cells were exposed to **17g** at concentrations of 0.1, 0.5, and 2.5 μM , the number of monomer forms (green fluorescence) gradually increased compared with the control group, while the number of aggregate forms (red fluorescence) gradually decreased. This change indicated that **17g** decreased the MMP in a dose-dependent manner. Furthermore, the results indicated that **17g** was able to induce MMP collapse and mitochondrial dysfunction, and downregulate the expression of antiapoptotic proteins, leading to A549 cell apoptosis.

2.2.7. Molecular docking

To investigate the possible binding mode of **17g**, a molecular docking study was performed at the colchicine site of tubulin (PDB code: 1SA0) [40]. The resulting binding mode is shown in Fig. 8A and

9B. As expected, **17g** occupied the colchicine binding site at the interface of α , β -tubulin, and was mostly confined in a deep pocket in β -tubulin opposite a GTP molecule bound in a pocket in α -tubulin (Fig. 8A). Specifically, the 3,4,5-trimethoxybenzene ring (A ring) of **17g** was buried deep within β -tubulin, while its benzo[b]furan ring (B ring) was facing α -tubulin, and the compound was tightly wrapped by the surrounding amino acid residues (Fig. 8B). The A ring penetrated into the hydrophobic pocket composed of Cys241, Val328, Tyr202, Leu255, and Ala354, and was involved in a hydrophobic interaction with Cys241. The benzo[b]furan sat deep in a pocket composed of Lys254, Val74, Gln11, Tyr224, and Asn101, and the 2-*N*-phenyl amide was positioned close to Ser178 and Val181. Altogether, compound **17g** exhibited efficient binding to the colchicine site of tubulin, which might support its inhibitory effect against tubulin.

3. Conclusion

In summary, we synthesized a series of novel 1-(benzofuran-3-yl)-1*H*-1,2,3-triazole derivatives as tubulin polymerization inhibitors. Compound **17g** showed the most potent antiproliferative activity and less toxicity among this series. Mechanistic studies indicated that **17g** inhibited tubulin polymerization, strongly disrupted microtubule organization in A549 cells, blocked the cell cycle in the G2/M phase by affecting cycle-related proteins, and led to apoptosis by downregulating

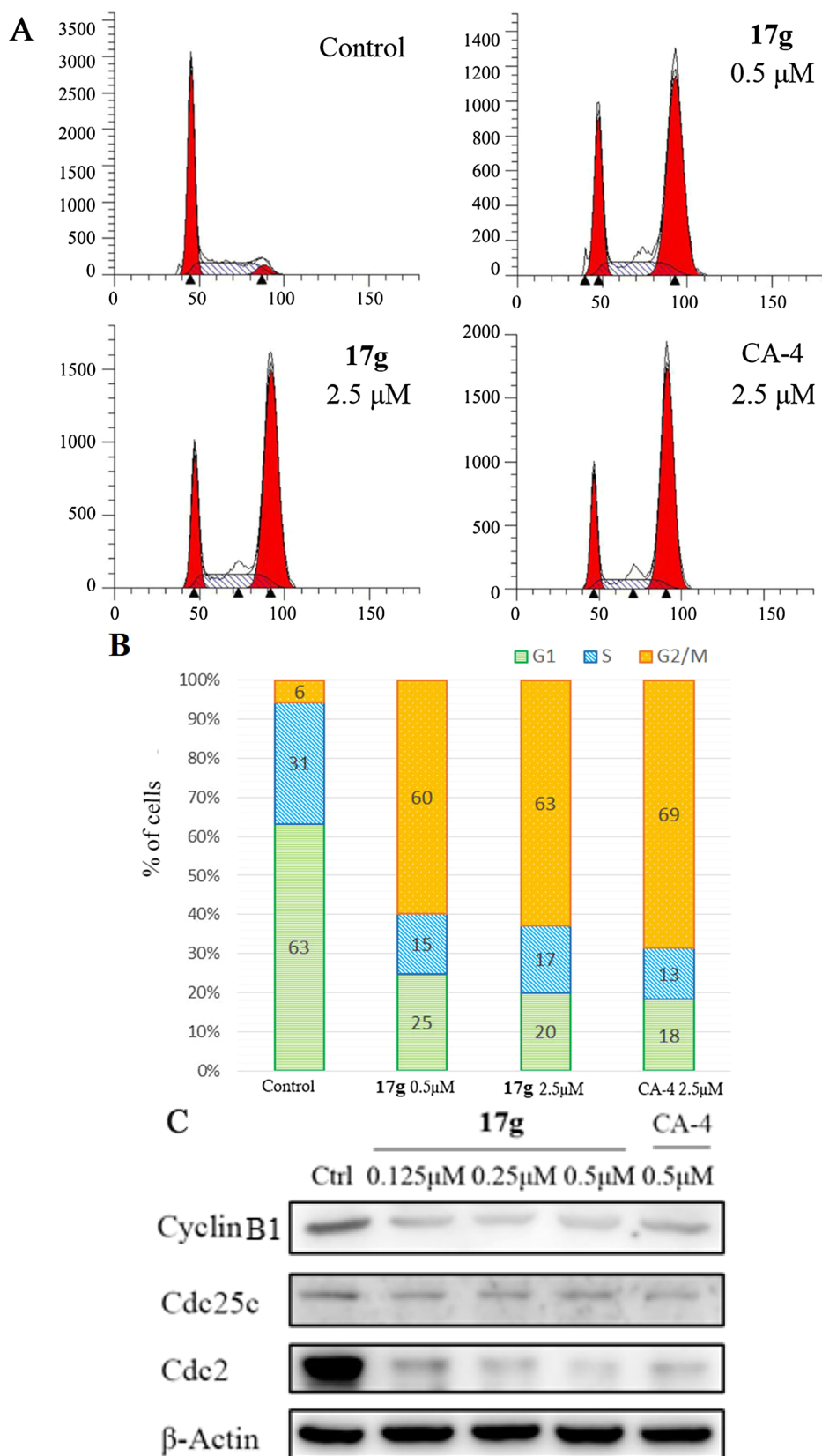


Fig. 5. (A) Effect of 17g on cell cycle arrest in A549 cells. A549 cells were treated with compound 17g and CA-4 at the indicated concentrations for 24 h. (B) Quantitative analysis of the percentage of cells in each cell cycle phase. (C) Expression of proteins cyclin B1, Cdc25c, and Cdc2 analyzed by Western blot.

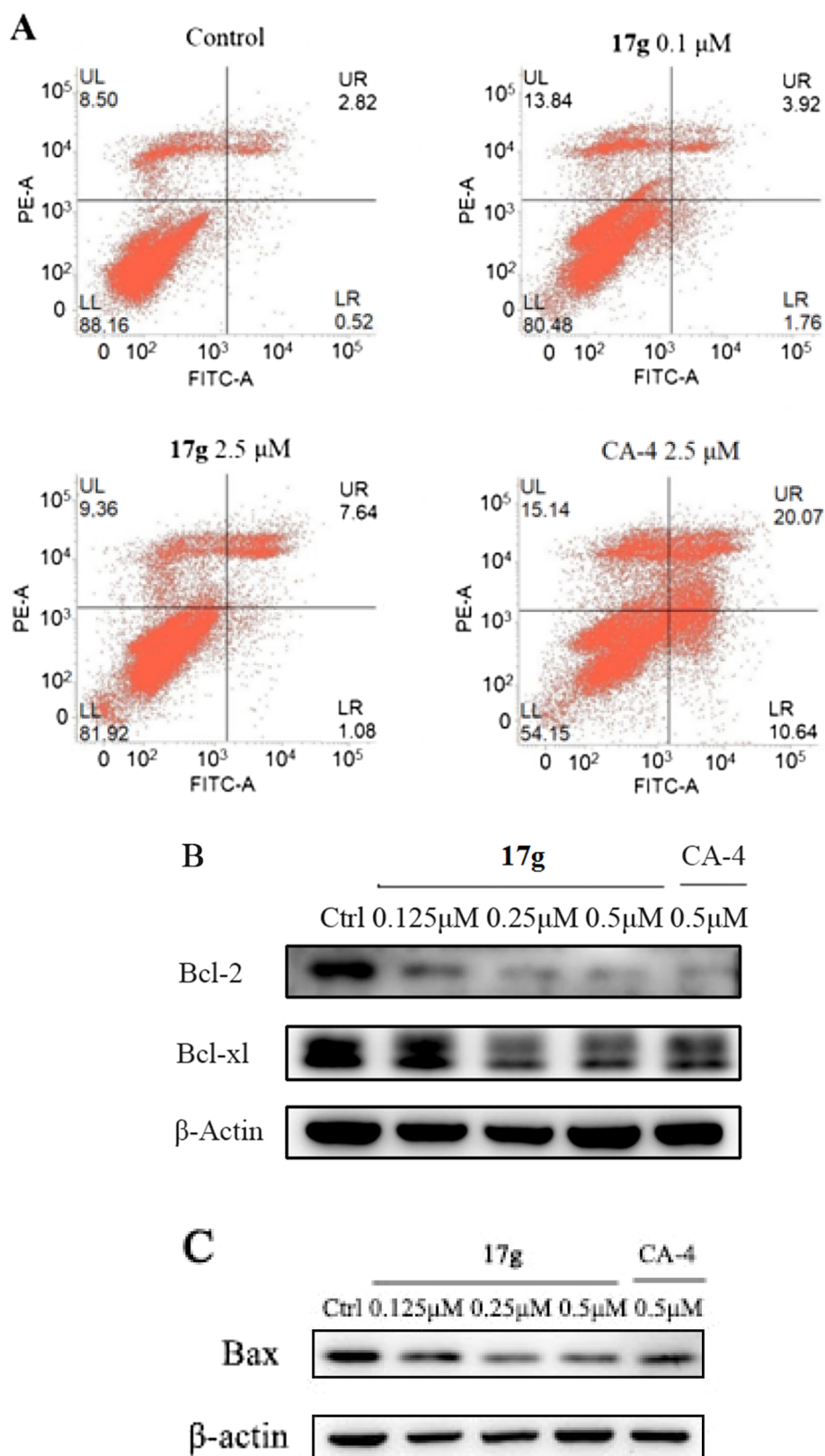


Fig. 6. (A) Effect of 17g on A549 cell apoptosis. A549 cells were treated with compound 17g and CA-4 at the indicated concentrations for 12 h. (B) Expression of proteins Bcl-2 and Bcl-xl analyzed by Western blot. (C) Expression of protein Bax analyzed by Western blot.

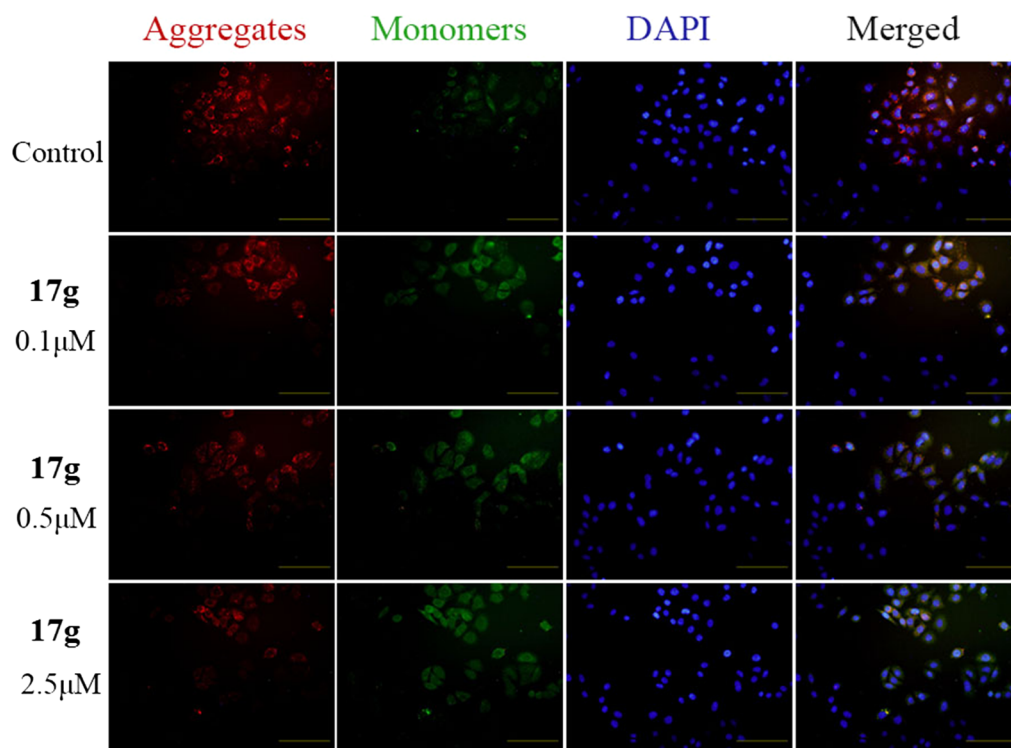


Fig. 7. Effect of **17g** on the MMP. A549 cells were treated with DMSO (0.01%) or **17g** at the indicated concentrations (0.1, 0.5 and 2.5 μM) for 6 h, followed by incubation with fluorescence probe JC-1 for 30 min. The cells were then analyzed by fluorescence microscopy. Scale bar: 10 μm .

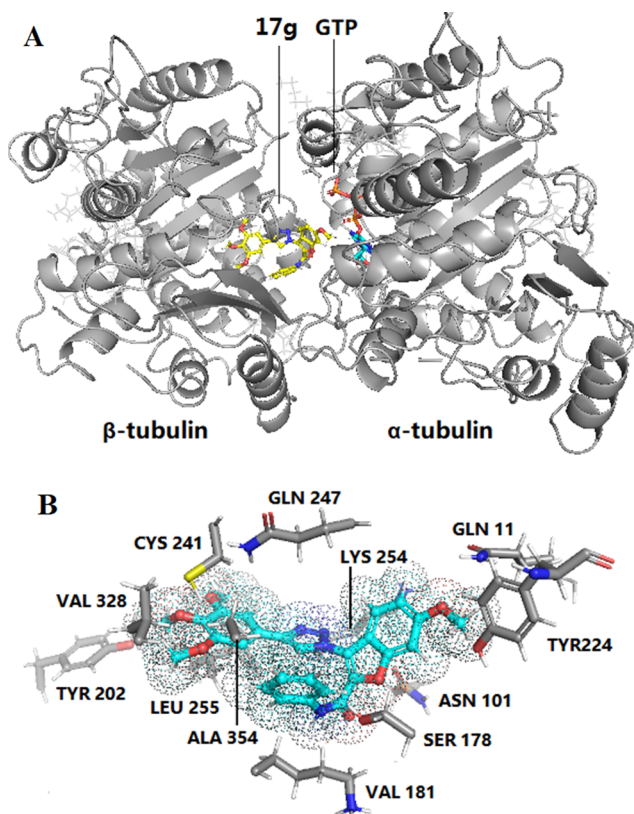


Fig. 8. Molecular docking of **17g** at the colchicine binding site of the α,β -tubulin interface. (A) Surface representation of **17g**. (B) **17g** (green sticks) and surrounding amino acid residues (gray sticks) of tubulin.

antiapoptotic proteins and decreasing the MMP of A549 cells. A docking study showed that **17g** was a good molecular fit at the colchicine binding site. Collectively, these results highlight that novel

tubulin polymerization inhibitor **17g** is a potential cancer treatment, warranting its further investigation and development.

4. Experiment

4.1. Chemistry

All starting materials and reagents were purchased commercially and used without further purified, unless otherwise stated. All reactions were monitored by thin layer chromatograph (TLC) on silica gel GF254 (0.25 mm thick). Column chromatography (CC) was performed on Silica Gel 60 (230–400 mesh, Qingdao Ocean Chemical Ltd., China). ^1H NMR and ^{13}C NMR spectra were recorded with Agilent NMR inova 600 or Bruker AM 400 spectrometers with TMS as an internal standard, all chemical shift values were reported as ppm. Mass spectra were recorded on a Bruker Dalton APEXII49e and Esquire 6000 (ESI-ION TRAP) spectrometer with ESI source as ionization, respectively.

4.1.1. 5-(2,2-Dibromovinyl)-1,2,3-trimethoxybenzene (**8**)

To a solution of CBr_4 (10 g, 15.3 mmol) in dry dichloromethane (50 mL) was slowly added PPh_3 (16 g, 30.6 mmol). The reaction mixture was stirred at room temperature for 1 h. Then added **7** (4.0 g, 10.2 mmol) at 0 $^\circ\text{C}$ and stirred for another 2 h. After the reaction was completed, the solid was filtered off, and the solution was concentrated under reduced pressure to give crude product. The crude product was purified by column chromatography (50:1 petroleum ether/ethyl acetate) to give 5-(2,2-dibromovinyl)-1,2,3-trimethoxybenzene **8** (3.7 g, yield 52%) as a yellow liquid. ^1H NMR (600 MHz, CDCl_3) δ 7.41 (s, 1H), 6.80 (s, 2H), 3.87 (s, 3H), 3.86 (s, 6H); MS (ESI) m/z 353.0 for $[\text{M} + \text{H}]^+$.

4.1.2. 5-Ethynyl-1,2,3-trimethoxybenzene (**9**)

To a solution of **8** (3.7 g, 10.5 mmol) in dry THF (50 mL) was slowly added $n\text{-BuLi}$ (12.5 mL, 31.5 mmol, 2.5 M in hexane) with a syringe at -78 $^\circ\text{C}$ under nitrogen protection. Stirring the mixture at -78 $^\circ\text{C}$ for

3 h and continue to react for 2 h at room temperature. After the reaction was finished, the mixture was quenched with saturated aqueous NH_4Cl , and the aqueous phase was extracted with Et_2O for three times. The combined organic extracts were dried over MgSO_4 , filtered, and concentrated under reduced pressure. Then the crude product was purified by column chromatography (100:1–60:1 petroleum ether/ethyl acetate) to give **9** (1.1 g, yield 55%) as a yellow solid. ^1H NMR (600 MHz, CDCl_3) δ 6.73 (s, 2H), 3.85 (s, 3H), 3.83 (s, 6H), 3.03 (s, 1H); MS (ESI) m/z 193.1 for $[\text{M}+\text{H}]^+$.

4.1.3. General procedures for preparation of compounds **11a,b**

To a solution of 2-hydroxybenzimidazole (8.0 g, 67.2 mmol) in DMF was added ethyl bromoacetate (13.5 g, 80.7 mmol) and K_2CO_3 (18.5 g, 134.4 mmol). The mixture was stirred at 60°C for 8 h, then heated to 140°C and stirred for 8 h. Then the mixture was added water (500 mL) and extracted with ethyl acetate. The combined organic extracts were dried over Na_2SO_4 , filtered, and concentrated under reduced pressure. The crude product was purified by column chromatography (10:1–6:1 petroleum ether/ethyl acetate) to give **11a**. A similar procedure was operated to provide pure **11b**.

4.1.3.1. *Ethyl 3-aminobenzofuran-2-carboxylate (11a)*. Yield: 73%; yellow solid; ^1H NMR (600 MHz, CDCl_3) δ 7.56 (d, $J = 7.8$ Hz, 1H), 7.46 (d, $J = 3.0$ Hz, 2H), 7.25 (s, 2H), 4.45 (q, $J = 7.2$ Hz, 2H), 1.44 (t, $J = 7.2$ Hz, 3H); MS (ESI) m/z 206.1 for $[\text{M}+\text{H}]^+$.

4.1.3.2. *Ethyl 3-amino-6-methoxybenzofuran-2-carboxylate (11b)*. Yield: 64%; yellow solid; ^1H NMR (600 MHz, $\text{DMSO}-d_6$) δ 7.78 (d, $J = 8.4$ Hz, 1H), 7.05 (d, $J = 1.8$ Hz, 1H), 6.85 (dd, $J = 6.6$ Hz, $J = 1.8$ Hz, 1H), 6.29 (brs, 2H), 4.24 (q, $J = 7.2$ Hz, 2H), 3.79 (s, 3H), 1.28 (t, $J = 7.2$ Hz, 3H). MS (ESI) m/z 236.1 for $[\text{M}+\text{H}]^+$.

4.1.4. General procedures for preparation of compounds **12a,b**

To a solution of **11a** (8.9 g, 43.4 mmol) in acetic acid (120 mL) and H_2O (12 mL) was added NaNO_2 (7.5 g, 108.5 mmol) and NaN_3 (7.0 g, 108.5 mmol) at 0°C . The reaction mixture was stirred at 0°C for 2.5 h. After the reaction was finished, the mixture was added aqueous NaHCO_3 (100 mL) and extracted with ethyl acetate. The combined organic extracts were dried over Na_2SO_4 , filtered, and concentrated under reduced pressure. Then the crude product was purified by column chromatography (20:1–10:1 petroleum ether/ethyl acetate) to give **12a**. A similar procedure was operated to provide pure **12b**.

4.1.4.1. *Ethyl 3-azidobenzofuran-2-carboxylate (12a)*. Yield: 47%; yellow solid; ^1H NMR (600 MHz, CDCl_3) δ 7.74 (d, $J = 8.4$ Hz, 1H), 7.55–7.49 (m, 2H), 7.32 (t, $J = 7.2$ Hz, 1H), 4.50 (q, $J = 7.2$ Hz, 2H), 1.46 (t, $J = 7.2$ Hz, 3H).

4.1.4.2. *Ethyl 3-azido-6-methoxybenzofuran-2-carboxylate (12b)*. Yield: 43%; yellow solid; ^1H NMR (600 MHz, CDCl_3) δ 7.57 (d, $J = 9.0$ Hz, 1H), 6.98 (d, $J = 1.8$ Hz, 1H), 6.93 (dd, $J = 7.2$, 1.8 Hz, 1H), 4.47 (q, $J = 7.2$ Hz, 2H), 3.86 (s, 3H), 1.44 (t, $J = 7.2$ Hz, 3H).

4.1.5. General procedures for preparation of compounds **13a,b**

To a solution of **12a** (4.7 g, 20 mmol) in THF (30 mL) and H_2O (1 mL) was added NaOH (4.9 g, 120 mmol). The reaction mixture was stirred at room temperature for 2 days. Then the reaction solution was acidified to $\text{pH} = 1$ by the dropwise addition of 3 M HCl and extracted with DCM. The combined organic extracts were dried over Na_2SO_4 , filtered, and concentrated under reduced pressure to give the product 3-azidobenzofuran-2-carboxylic acid (**13a**). A similar procedure was operated to provide 3-azido-6-methoxybenzofuran-2-carboxylic acid **13b**. These two compounds were directly used in next reaction without further purification.

4.1.6. General procedures for preparation of compounds **14b** and **15b**

To a solution of **13a** (0.25 g, 1.23 mmol) in DCM (20 mL) was added $\text{EDC}\cdot\text{HCl}$ (0.35 g, 1.89 mmol), DMAP (0.03 g, 0.25 mmol) and isopropanol (1.0 mL). The reaction mixture was stirred at room temperature for 24 h. Then the mixture was added H_2O (50 mL) and extracted with DCM. The combined organic extracts were dried over Na_2SO_4 , filtered, and concentrated under reduced pressure. Then the crude product was purified by column chromatography (50:1–20:1 petroleum ether/ethyl acetate) to give **14b**. A similar procedure was operated to provide pure compound **15b**.

4.1.6.1. *Isopropyl 3-azidobenzofuran-2-carboxylate (14b)*. Yield: 70%; yellow solid; ^1H NMR (600 MHz, CDCl_3) δ 7.73 (d, $J = 8.4$ Hz, 1H), 7.54 (d, $J = 8.4$ Hz, 1H), 7.50 (t, $J = 8.4$ Hz, 1H), 7.33 (t, $J = 7.8$ Hz, 1H), 5.39–5.37 (m, 1H), 1.45 (d, $J = 6.0$ Hz, 6H).

4.1.6.2. *Isopropyl 3-azido-6-methoxybenzofuran-2-carboxylate (15b)*. Yield: 76%; yellow solid; ^1H NMR (600 MHz, CDCl_3) δ 7.57 (d, $J = 9.0$ Hz, 1H), 6.99 (s, 1H), 6.93 (d, $J = 9.0$ Hz, 1H), 5.36–5.35 (m, 1H), 3.86 (s, 3H), 1.44 (d, $J = 9.6$ Hz, 6H).

4.1.7. General procedures for preparation of compounds **14c-i**, **15c-i**

To a solution of **13a** (0.24 g, 1.18 mmol) in DCM (20 mL) was added $\text{EDC}\cdot\text{HCl}$ (0.29 g, 1.54 mmol), HOBt (0.21 g, 1.54 mmol) and propylamine (1.0 mL). The reaction mixture was stirred at room temperature for overnight. After the reaction was finished, the mixture was added H_2O (50 mL) and extracted with DCM. The combined organic extracts were dried over Na_2SO_4 , filtered, and concentrated under reduced pressure. Then the crude product was purified by column chromatography (50:1–20:1 petroleum ether/ethyl acetate) to give **14c**. Similar procedures were operated to provide pure compounds **14d-i**, **15c-i**.

4.1.7.1. *3-Azido-N-propylbenzofuran-2-carboxamide (14c)*. Yield: 79%; yellow solid; ^1H NMR (600 MHz, CDCl_3) δ 7.73 (d, $J = 8.4$ Hz, 1H), 7.49–7.45 (m, 2H), 7.32 (t, $J = 7.8$ Hz, 1H), 6.65 (brs, 1H), 3.46 (q, $J = 6.6$ Hz, 2H), 1.69–1.66 (m, 2H), 1.01 (t, $J = 7.2$ Hz, 3H).

4.1.7.2. *3-Azido-N-cyclopropylbenzofuran-2-carboxamide (14d)*. Yield: 42%; yellow solid; ^1H NMR (600 MHz, CDCl_3) δ 7.72 (d, $J = 8.4$ Hz, 1H), 7.47 (d, $J = 3.6$ Hz, 2H), 7.33–7.30 (m, 1H), 6.71 (brs, 1H), 2.95–2.92 (m, 1H), 0.91 (q, $J = 6.0$ Hz, 2H), 0.70–0.67 (m, 2H).

4.1.7.3. *3-Azido-N-cyclopentylbenzofuran-2-carboxamide (14e)*. Yield: 40%; yellow solid; ^1H NMR (600 MHz, CDCl_3) δ 7.72 (d, $J = 7.8$ Hz, 1H), 7.49–7.45 (m, 2H), 7.31 (t, $J = 7.8$ Hz, 1H), 6.56 (brs, 1H), 4.45–4.42 (m, 1H), 2.10 (t, $J = 6.0$ Hz, 2H), 1.80–1.76 (m, 2H), 1.7–1.68 (m, 2H), 1.60–1.55 (m, 2H).

4.1.7.4. *3-Azido-N-cyclohexylbenzofuran-2-carboxamide (14f)*. Yield: 84%; yellow solid; ^1H NMR (600 MHz, CDCl_3) δ 7.72 (d, $J = 8.4$ Hz, 1H), 7.49–7.45 (m, 2H), 7.33–7.30 (m, 1H), 6.56 (d, $J = 7.8$ Hz, 1H), 4.03–4.02 (m, 1H), 2.05 (dd, $J = 9.0$, 3.6 Hz, 2H), 1.77 (dt, $J = 13.8$, 3.6 Hz, 2H), 1.67 (dd, $J = 9.6$, 4.2 Hz, 1H), 1.47–1.41 (m, 2H), 1.35–1.22 (m, 4H).

4.1.7.5. *3-Azido-N-phenylbenzofuran-2-carboxamide (14g)*. Yield: 80%; yellow solid; ^1H NMR (600 MHz, CDCl_3) δ 8.36 (brs, 1H), 7.78 (d, $J = 7.8$ Hz, 1H), 7.71 (d, $J = 7.8$ Hz, 2H), 7.56–7.50 (m, 2H), 7.41–7.35 (m, 3H), 7.17 (t, $J = 7.8$ Hz, 1H).

4.1.7.6. *(3-Azidobenzofuran-2-yl)(piperidin-1-yl)methanone (14h)*. Yield: 76%; yellow solid; ^1H NMR (600 MHz, CDCl_3) δ 7.68 (d, $J = 7.8$ Hz, 1H), 7.45–7.39 (m, 2H), 7.27 (t, $J = 7.2$ Hz, 1H), 3.68 (s, 2H), 3.64 (s, 2H), 1.70–1.65 (m, 6H).

4.1.7.7. *(3-Azidobenzofuran-2-yl)(piperidin-1-yl)methanone*

(14i). Yield: 76%; yellow solid; ^1H NMR (600 MHz, CDCl_3) δ 7.72 (d, $J = 7.8$ Hz, 1H), 7.47–7.45 (m, 2H), 7.32 (t, $J = 6.0$ Hz, 1H), 3.80 (brs, 8H).

4.1.7.8. 3-Azido-6-methoxy-N-propylbenzofuran-2-carboxamide (15c). Yield: 68%; yellow solid; ^1H NMR (600 MHz, CDCl_3) δ 7.58 (d, $J = 8.4$ Hz, 1H), 6.96 (s, 1H), 6.94 (d, $J = 9.0$ Hz, 1H), 6.56 (brs, 1H), 3.87 (s, 3H), 3.44 (q, $J = 6.6$ Hz, 2H), 1.68–1.64 (m, 2H), 1.00 (t, $J = 7.2$ Hz, 3H).

4.1.7.9. 3-Azido-N-cyclopropyl-6-methoxybenzofuran-2-carboxamide (15d). Yield: 74%; yellow solid; ^1H NMR (600 MHz, CDCl_3) δ 7.57 (d, $J = 9.6$ Hz, 1H), 6.94–6.92 (m, 2H), 6.63 (brs, 1H), 3.86 (s, 3H), 2.92–2.90 (m, 1H), 0.90–0.86 (m, 2H), 0.66 (s, 2H).

4.1.7.10. 3-Azido-N-cyclopentyl-6-methoxybenzofuran-2-carboxamide (15e). Yield: 68%; yellow solid; ^1H NMR (600 MHz, CDCl_3) δ 7.71 (d, $J = 3.6$ Hz, 1H), 6.95 (s, 1H), 6.93 (d, $J = 9.0$ Hz, 1H), 6.48 (d, $J = 6.0$ Hz, 1H), 4.43 (q, $J = 7.2$ Hz, 1H), 3.86 (s, 3H), 2.10 (q, $J = 6.0$ Hz, 2H), 1.76–1.70 (m, 2H), 1.69–1.66 (m, 2H), 1.55–1.51 (m, 2H).

4.1.7.11. 3-Azido-N-cyclohexyl-6-methoxybenzofuran-2-carboxamide (15f). Yield: 69%; yellow solid; ^1H NMR (600 MHz, CDCl_3) δ 7.57 (d, $J = 8.4$ Hz, 1H), 6.96 (s, 1H), 6.93 (d, $J = 7.8$ Hz, 1H), 6.42 (d, $J = 6.6$ Hz, 1H), 4.02–4.00 (m, 1H), 3.87 (s, 3H), 2.04–2.02 (m, 2H), 1.78–1.71 (m, 2H), 1.67–1.64 (m, 1H), 1.46–1.41 (m, 2H), 1.33–1.25 (m, 3H).

4.1.7.12. 3-Azido-6-methoxy-N-phenylbenzofuran-2-carboxamide (15g). Yield: 66%; yellow solid; ^1H NMR (600 MHz, CDCl_3) δ 8.27 (brs, 1H), 7.69 (d, $J = 7.8$ Hz, 2H), 7.63 (d, $J = 9.6$ Hz, 1H), 7.38 (d, $J = 7.8$ Hz, 2H), 7.17 (d, $J = 7.2$ Hz, 1H), 7.01 (s, 1H), 6.97 (d, $J = 8.4$ Hz, 1H), 3.89 (s, 3H).

4.1.7.13. (3-Azido-6-methoxybenzofuran-2-yl)(piperidin-1-yl)methanone (15h). Yield: 68%; yellow solid; ^1H NMR (600 MHz, CDCl_3) δ 7.56 (d, $J = 9.0$ Hz, 1H), 6.94–6.91 (m, 2H), 3.86 (s, 3H), 3.67 (brs, 4H), 1.71–1.67 (m, 6H).

4.1.7.14. (3-Azido-6-methoxybenzofuran-2-yl)(morpholino)methanone (15i). Yield: 68%; yellow solid; ^1H NMR (600 MHz, CDCl_3) δ 7.58 (d, $J = 4.2$ Hz, 1H), 6.94–6.93 (m, 2H), 3.88 (s, 3H), 3.79 (brs, 8H).

4.1.8. General procedures for preparation of compounds 16a-i, 17a-i

To a solution of **9** (0.24 g, 1.18 mmol) in *t*-BuOH (10 mL) and H_2O (10 mL) was added $\text{CuSO}_4 \cdot 5\text{H}_2\text{O}$ (0.29 g, 1.54 mmol), sodium ascorbate (0.21 g, 1.54 mmol) and **12a** (0.13 g, 0.58 mmol). The reaction mixture was stirred at room temperature for overnight. Then the mixture was added 3 M HCl (100 mL) and extracted with CHCl_3 . The combined organic extracts were dried over Na_2SO_4 , filtered, and concentrated under reduced pressure. Then the crude product was purified by column chromatography (10:1–2:1 petroleum ether/ethyl acetate) to give **16a**. Similar procedures were operated to provide pure compounds **16b-i**, **17a-i**.

4.1.8.1. Ethyl-3-(4-(3,4,5-trimethoxyphenyl)-1H-1,2,3-triazol-1-yl)benzofuran-2-carboxylate (16a). Yield: 79%; yellow solid; m.p.: 168–170 °C; ^1H NMR (600 MHz, CDCl_3) δ 8.78 (s, 1H), 8.14 (d, $J = 8.4$ Hz, 1H), 7.65 (d, $J = 8.4$ Hz, 1H), 7.59 (t, $J = 8.4$ Hz, 1H), 7.44 (t, $J = 7.8$ Hz, 1H), 7.19 (s, 2H), 4.48 (q, $J = 7.2$ Hz, 2H), 3.97 (s, 6H), 3.91 (s, 3H), 1.43 (t, $J = 7.2$ Hz, 3H); ^{13}C NMR (150 MHz, CDCl_3) δ 158.6, 153.8 (2C), 153.5, 147.0, 138.7, 134.5, 129.4, 125.6, 125.5, 124.9, 123.3, 122.8, 122.3, 112.4, 103.5 (2C), 62.2, 60.9, 56.3 (2C), 14.1; MS (ESI) m/z 424.2 for $[\text{M}+1]^+$; HRMS (ESI) 424.1511 for $[\text{M}+1]^+$ (calcd 424.1503 for $\text{C}_{22}\text{H}_{22}\text{N}_3\text{O}_6$); HPLC purity > 99%

(MeOH:H₂O = 80:20, 0.5 mL/min, $t_R = 8.71$ min).

4.1.8.2. Isopropyl 3-(4-(3,4,5-trimethoxyphenyl)-1H-1,2,3-triazol-1-yl)benzofuran-2-carboxylate (16b). Yield: 65%; yellow solid; m.p.: 171–173 °C; ^1H NMR (400 MHz, CDCl_3) δ 8.65 (s, 1H), 8.04 (d, $J = 8.0$ Hz, 1H), 7.60 (d, $J = 8.0$ Hz, 1H), 7.53 (t, $J = 8.0$ Hz, 1H), 7.38 (t, $J = 8.0$ Hz, 1H), 7.12 (s, 2H), 5.27 (p, $J = 4.0$ Hz, 1H), 3.90 (s, 6H), 3.84 (s, 3H), 1.33 (d, $J = 4.0$ Hz, 6H); ^{13}C NMR (150 MHz, CDCl_3) δ 158.1, 153.8 (2C), 153.5, 138.6, 135.2, 129.2, 125.7, 124.9 (2C), 123.1 (2C), 122.8, 112.4 (2C), 103.3 (2C), 70.3, 60.9, 56.3 (2C), 21.8 (2C); MS (ESI) m/z 438.2 for $[\text{M}+1]^+$; HRMS (ESI) 438.1668 for $[\text{M}+1]^+$ (calcd 438.1660 for $\text{C}_{23}\text{H}_{24}\text{N}_3\text{O}_6$); HPLC purity 98.7% (MeOH:H₂O = 75:25, 0.8 mL/min, $t_R = 7.96$ min).

4.1.8.3. N-propyl-3-(4-(3,4,5-trimethoxyphenyl)-1H-1,2,3-triazol-1-yl)benzofuran-2-carboxamide (16c). Yield: 70%; yellow solid; m.p.: 167–169 °C; ^1H NMR (400 MHz, CDCl_3) δ 9.24 (s, 1H), 8.32 (d, $J = 8.0$ Hz, 1H), 7.57 (d, $J = 4.0$ Hz, 2H), 7.45 (dt, $J = 8.2$, 4.1 Hz, 1H), 7.21 (s, 2H), 6.99 (s, 1H), 3.97 (s, 6H), 3.91 (s, 3H), 3.49 (q, $J = 6.8$ Hz, 2H), 1.77–1.67 (m, 2H), 1.04 (t, $J = 8.0$ Hz, 3H); ^{13}C NMR (150 MHz, CDCl_3) δ 158.1, 153.7 (2C), 152.5, 146.8, 138.5, 136.0, 128.6, 125.8, 124.9, 124.1 (2C), 123.0 (2C), 111.7, 103.6 (2C), 60.9, 56.4 (2C), 41.3, 22.8, 11.4; MS (ESI) m/z 437.1 for $[\text{M}+1]^+$; HRMS (ESI) 437.1832 for $[\text{M}+1]^+$ (calcd 437.1819 for $\text{C}_{23}\text{H}_{25}\text{N}_4\text{O}_5$); HPLC purity 98.5% (MeOH:H₂O = 35:65, 0.8 mL/min, $t_R = 4.21$ min).

4.1.8.4. N-cyclopropyl-3-(4-(3,4,5-trimethoxyphenyl)-1H-1,2,3-triazol-1-yl)benzofuran-2-carboxamide (16d). Yield: 65%; yellow solid; m.p.: 175–176 °C; ^1H NMR (600 MHz, CDCl_3) δ 9.30 (s, 1H), 8.34 (d, $J = 8.4$ Hz, 1H), 7.57–7.53 (m, 2H), 7.44 (t, $J = 7.2$ Hz, 1H), 7.22 (s, 2H), 7.05 (s, 1H), 3.95 (s, 6H), 3.91 (s, 3H), 2.95 (d, $J = 3.0$ Hz, 1H), 0.97 (d, $J = 6.6$ Hz, 2H), 0.75 (s, 2H); ^{13}C NMR (150 MHz, CDCl_3) δ 159.5, 153.7 (2C), 152.4, 146.7, 138.6, 135.5, 128.7, 125.8, 124.8, 124.2, 123.2, 123.0, 122.9, 111.6, 103.5, 103.4, 60.8, 56.3 (2C), 29.6, 22.6, 6.7; MS (ESI) m/z 435.2 for $[\text{M}+1]^+$; HRMS (ESI) 435.1671 for $[\text{M}+1]^+$ (calcd 435.1663 for $\text{C}_{23}\text{H}_{23}\text{N}_4\text{O}_5$); HPLC purity > 99% (MeOH:H₂O = 35:65, 0.8 mL/min, $t_R = 4.38$ min).

4.1.8.5. N-cyclopentyl-3-(4-(3,4,5-trimethoxyphenyl)-1H-1,2,3-triazol-1-yl)benzofuran-2-carboxamide (16e). Yield: 75%; yellow solid; m.p.: 178–180 °C; ^1H NMR (600 MHz, CDCl_3) δ 9.25 (s, 1H), 8.30 (d, $J = 7.8$ Hz, 1H), 7.57 (s, 2H), 7.43 (t, $J = 6.0$ Hz, 1H), 7.21 (s, 2H), 6.93 (d, $J = 7.2$ Hz, 1H), 4.44 (q, $J = 7.2$ Hz, 1H), 3.98 (s, 6H), 3.91 (s, 3H), 2.14 (q, $J = 6.0$ Hz, 2H), 1.81 (s, 2H), 1.72–1.70 (m, 2H), 1.64–1.59 (m, 2H); ^{13}C NMR (150 MHz, CDCl_3) δ 157.7, 153.7 (2C), 152.4, 146.8, 138.6, 136.1, 128.6, 125.9, 124.9, 124.1 (2C), 123.0 (2C), 111.7, 103.6 (2C), 60.9, 56.4 (2C), 51.4, 33.2 (2C), 23.8 (2C); MS (ESI) m/z 463.2 for $[\text{M}+1]^+$; HRMS (ESI) 463.1982 for $[\text{M}+1]^+$ (calcd 463.1976 for $\text{C}_{25}\text{H}_{27}\text{N}_4\text{O}_6$); HPLC purity 97.2% (MeOH:H₂O = 45:55, 0.8 mL/min, $t_R = 4.10$ min).

4.1.8.6. N-cyclohexyl-3-(4-(3,4,5-trimethoxyphenyl)-1H-1,2,3-triazol-1-yl)benzofuran-2-carboxamide (16f). Yield: 63%; yellow solid; m.p.: 176–178 °C; ^1H NMR (400 MHz, CDCl_3) δ 9.16 (s, 1H), 8.23 (d, $J = 8.0$ Hz, 1H), 7.53–7.44 (m, 2H), 7.37 (td, $J = 8.2$, 6.9, 4.2 Hz, 1H), 7.14 (s, 2H), 6.75 (d, $J = 8.0$ Hz, 1H), 3.93 (s, 1H), 3.90 (s, 6H), 3.83 (s, 3H), 2.02–1.97 (m, 2H), 1.64–1.60 (m, 3H), 1.43–1.27 (m, 3H); ^{13}C NMR (150 MHz, CDCl_3) δ 157.2, 153.7 (2C), 152.4, 146.8, 138.5, 136.1, 128.6, 125.9, 124.9, 124.1, 123.1 (2C), 123.0, 111.7, 103.5 (2C), 60.9, 56.4 (2C), 48.6, 33.1 (2C), 25.4 (2C), 24.8; MS (ESI) m/z 477.2 for $[\text{M}+1]^+$; HRMS (ESI) 477.2142 for $[\text{M}+1]^+$ (calcd 477.2132 for $\text{C}_{26}\text{H}_{29}\text{N}_4\text{O}_5$); HPLC purity > 99% (MeOH:H₂O = 50:50, 0.8 mL/min, $t_R = 4.20$ min).

4.1.8.7. N-phenyl-3-(4-(3,4,5-trimethoxyphenyl)-1H-1,2,3-triazol-1-yl)benzofuran-2-carboxamide (16g). Yield: 60%; yellow solid; m.p.:

175–177 °C; ^1H NMR (600 MHz, CDCl_3) δ 9.18 (s, 1H), 8.71 (s, 1H), 8.33 (d, $J = 7.8$ Hz, 1H), 7.71 (d, $J = 7.8$ Hz, 1H), 7.64–7.62 (m, 2H), 7.49 (d, $J = 8.4$ Hz, 2H), 7.43 (t, $J = 7.8$ Hz, 2H), 7.23 (s, 1H), 7.21 (s, 2H) 3.98 (s, 6H), 3.91 (s, 3H); ^{13}C NMR (150 MHz, CDCl_3) δ 156.0, 153.7 (2C), 152.6, 147.1, 136.7, 135.7, 129.3 (2C), 129.2, 125.7, 125.5, 125.2, 124.2, 124.1, 123.1, 122.9, 120.6 (2C), 112.0 (2C), 103.5 (2C), 61.0, 56.4 (2C); MS (ESI) m/z 471.1 for $[\text{M}+1]^+$; HRMS (ESI) 471.1676 for $[\text{M}+\text{H}]^+$ (calcd 471.1663 for $\text{C}_{26}\text{H}_{23}\text{N}_4\text{O}_5$); HPLC purity > 99% (MeOH:H₂O = 60:40, 0.8 mL/min, $t_R = 4.09$ min).

4.1.8.8. Piperidin-1-yl(3-(4-(3,4,5-trimethoxyphenyl)-1H-1,2,3-triazol-1-yl)benzofuran-2-yl)methanone (16h). Yield: 61%; yellow solid; m.p.: 182–184 °C; ^1H NMR (600 MHz, CDCl_3) δ 8.67 (s, 1H), 8.07 (d, $J = 8.4$ Hz, 1H), 7.59 (d, $J = 8.4$ Hz, 1H), 7.52 (t, $J = 7.2$ Hz, 1H), 7.43 (t, $J = 7.8$ Hz, 1H), 7.17 (s, 2H), 3.97 (s, 6H), 3.90 (s, 3H), 3.73 (s, 2H), 3.43 (s, 2H), 1.69 (s, 4H), 1.59 (s, 2H); ^{13}C NMR (600 MHz, CDCl_3) δ 158.7, 153.7 (2C), 152.8, 147.4, 139.3, 138.4, 127.6, 125.7, 124.8, 122.5, 122.0, 121.7, 121.0, 112.0, 103.2 (2C), 61.0, 56.3 (2C), 48.2, 43.7, 26.5, 25.5, 24.3; MS (ESI) m/z 463.2 for $[\text{M}+1]^+$; HRMS (ESI) 463.1989 for $[\text{M}+\text{H}]^+$ (calcd 463.1976 for $\text{C}_{25}\text{H}_{27}\text{N}_4\text{O}_5$); HPLC purity > 99% (MeOH:H₂O = 40:60, 0.8 mL/min, $t_R = 4.41$ min).

4.1.8.9. Morpholino(3-(4-(3,4,5-trimethoxyphenyl)-1H-1,2,3-triazol-1-yl)benzofuran-2-yl)methanone (16i). Yield: 76%; yellow solid; m.p.: 178–180 °C; ^1H NMR (600 MHz, CDCl_3) δ 8.72 (s, 1H), 8.06 (d, $J = 8.4$ Hz, 1H), 7.60 (d, $J = 8.4$ Hz, 1H), 7.54 (t, $J = 7.2$ Hz, 1H), 7.44 (t, $J = 7.2$ Hz, 1H), 7.18 (s, 2H), 3.97 (s, 6H), 3.91 (s, 3H), 3.80 (s, 4H), 3.70 (s, 2H), 3.60 (s, 2H); ^{13}C NMR (600 MHz, CDCl_3) δ 158.8, 153.7 (2C), 152.7, 147.4, 138.4, 138.2, 128.0, 125.5, 125.0, 122.3 (2C), 122.1, 121.8, 112.0, 103.2 (2C), 66.7, 66.5, 60.9, 56.3 (2C), 47.4, 43.0; MS (ESI) m/z 465.2 for $[\text{M}+1]^+$; HRMS (ESI) 465.1777 for $[\text{M}+\text{H}]^+$ (calcd 465.1769 for $\text{C}_{24}\text{H}_{25}\text{N}_4\text{O}_6$); HPLC purity > 99% (MeOH:H₂O = 50:50, 0.8 mL/min, $t_R = 4.18$ min).

4.1.8.10. Ethyl 6-methoxy-3-(4-(3,4,5-trimethoxyphenyl)-1H-1,2,3-triazol-1-yl)benzofuran-2-carboxylate (17a). Yield: 61%; yellow solid; m.p.: 169–171 °C; ^1H NMR (400 MHz, CDCl_3) δ 8.86 (s, 1H), 8.06 (d, $J = 8.8$ Hz, 1H), 7.19 (s, 2H), 7.12–7.03 (m, 2H), 4.47 (q, $J = 8.0$ Hz, 2H), 3.97 (s, 6H), 3.91 (s, 3H), 3.90 (s, 3H), 1.44 (t, $J = 8.0$ Hz, 3H); ^{13}C NMR (150 MHz, CDCl_3) δ 161.9, 158.7, 155.1, 153.8 (2C), 147.0, 138.6, 133.2, 126.1, 125.7, 124.1, 122.3, 115.9, 115.5, 103.4 (2C), 95.4, 62.0, 60.9, 56.4 (2C), 55.8, 14.2; MS (ESI) m/z 454.2 for $[\text{M}+1]^+$; HRMS (ESI) 454.1623 for $[\text{M}+\text{H}]^+$ (calcd 454.1609 for $\text{C}_{23}\text{H}_{24}\text{N}_3\text{O}_7$); HPLC purity > 99% (MeOH:H₂O = 50:50, 0.8 mL/min, $t_R = 4.23$ min).

4.1.8.11. Isopropyl 6-methoxy-3-(4-(3,4,5-trimethoxyphenyl)-1H-1,2,3-triazol-1-yl)benzofuran-2-carboxylate (17b). Yield: 61%; yellow solid; m.p.: 171–173 °C; ^1H NMR (400 MHz, CDCl_3) δ 8.75 (s, 1H), 7.94 (d, $J = 8.0$ Hz, 1H), 7.08 (s, 2H), 7.02 (d, $J = 4.0$ Hz, 1H), 6.98 (q, $J = 4.0$ Hz, 1H), 5.26 (p, $J = 8.0$ Hz, 1H), 3.90 (s, 6H), 3.84 (s, 6H), 1.33 (d, $J = 8.0$ Hz, 6H); ^{13}C NMR (150 MHz, CDCl_3) δ 161.8, 158.2, 155.1, 153.8 (2C), 138.7, 133.8, 125.7, 123.8 (2C), 116.1, 115.4 (2C), 103.4 (2C), 95.5 (2C), 70.0, 60.9, 56.3 (2C), 55.8, 21.8 (2C); MS (ESI) m/z 468.2 for $[\text{M}+1]^+$; HRMS (ESI) 468.1779 for $[\text{M}+\text{H}]^+$ (calcd 468.1765 for $\text{C}_{24}\text{H}_{26}\text{N}_3\text{O}_7$); HPLC purity > 99% (MeOH:H₂O = 35:65, 0.8 mL/min, $t_R = 4.53$ min).

4.1.8.12. 6-Methoxy-N-propyl-3-(4-(3,4,5-trimethoxyphenyl)-1H-1,2,3-triazol-1-yl)benzofuran-2-carboxamide (17c). Yield: 63%; yellow solid; m.p.: 169–171 °C; ^1H NMR (400 MHz, CDCl_3) δ 9.33 (s, 1H), 8.22 (d, $J = 8.0$ Hz, 1H), 7.20 (s, 2H), 7.12–6.96 (m, 2H), 6.88 (s, 1H), 3.97 (s, 6H), 3.91 (s, 3H), 3.90 (s, 3H), 3.47 (q, $J = 8.0$ Hz, 2H), 1.70 (s, 2H), 1.04 (t, $J = 8.0$ Hz, 3H); ^{13}C NMR (150 MHz, CDCl_3) δ 161.2, 158.2, 153.8, 153.6, 146.7, 134.9, 125.9, 124.6, 123.3, 122.9, 116.2, 114.5 (2C), 103.5 (2C), 95.4 (2C), 60.9, 56.3 (2C), 55.8, 40.1, 22.8, 11.3; MS

(ESI) m/z 467.2 for $[\text{M}+1]^+$; HRMS (ESI) 467.1936 for $[\text{M}+\text{H}]^+$ (calcd 467.1925 for $\text{C}_{24}\text{H}_{28}\text{N}_4\text{O}_6$); HPLC purity > 99% (MeOH:H₂O = 20:80, 0.8 mL/min, $t_R = 4.25$ min).

4.1.8.13. N-Cyclopropyl-6-methoxy-3-(4-(3,4,5-trimethoxyphenyl)-1H-1,2,3-triazol-1-yl)benzofuran-2-carboxamide (17d). Yield: 65%; yellow solid; m.p.: 174–176 °C; ^1H NMR (400 MHz, CDCl_3) δ 9.31 (s, 1H), 8.15 (q, 4.0 Hz, 1H), 7.14 (s, 2H), 6.96 (dt, $J = 8.9, 2.3$ Hz, 1H), 6.92–6.86 (m, 2H), 3.90 (d, $J = 1.5$ Hz, 6H), 3.81 (s, 3H), 3.80 (s, 3H), 2.91–2.81 (m, 1H), 0.87 (q, $J = 4.0$ Hz, 2H), 0.69–0.62 (m, 2H); ^{13}C NMR (150 MHz, CDCl_3) δ 161.3, 159.7, 153.8, 153.6, 146.7, 138.3, 134.3, 125.9, 124.9, 123.6, 122.9, 116.0, 114.6, 103.3 (2C), 95.2 (2C), 60.9, 56.3 (2C), 55.8, 22.6, 6.8 (2C); MS (ESI) m/z 465.2 for $[\text{M}+1]^+$; HRMS (ESI) 465.1779 for $[\text{M}+\text{H}]^+$ (calcd 465.1769 for $\text{C}_{24}\text{H}_{25}\text{N}_4\text{O}_6$); HPLC purity > 99% (MeOH:H₂O = 50:50, 0.8 mL/min, $t_R = 4.16$ min).

4.1.8.14. N-Cyclopentyl-6-methoxy-3-(4-(3,4,5-trimethoxyphenyl)-1H-1,2,3-triazol-1-yl)benzofuran-2-carboxamide (17e). Yield: 70%; yellow solid; m.p.: 171–173 °C; ^1H NMR (600 MHz, CDCl_3) δ 9.33 (s, 1H), 8.22 (d, $J = 9.0$ Hz, 1H), 7.21 (s, 2H), 7.20 (s, 2H), 7.06 (dd, $J = 7.2, 1.8$ Hz, 1H), 7.03 (d, $J = 2.4$ Hz, 1H), 6.78 (d, $J = 7.8$ Hz, 1H), 4.44–4.42 (m, 1H), 3.97 (s, 6H), 3.91 (s, 1H), 3.90 (s, 1H), 2.13 (dd, $J = 7.2, 6.0$ Hz, 2H), 1.82–1.79 (m, 2H), 1.72–1.70 (m, 2H), 1.62–1.57 (m, 2H); ^{13}C NMR (150 MHz, CDCl_3) δ 161.1, 157.8, 153.8, 153.6, 146.7, 138.3, 134.9, 125.9, 124.7, 123.3, 122.9, 116.2, 114.5, 103.4 (2C), 95.3 (2C), 60.9, 56.3 (2C), 55.8, 51.3, 33.2 (2C), 23.8 (2C); MS (ESI) m/z 493.2 for $[\text{M}+1]^+$; HRMS (ESI) 493.2094 for $[\text{M}+\text{H}]^+$ (calcd 493.2080 for $\text{C}_{26}\text{H}_{29}\text{N}_4\text{O}_6$); HPLC purity > 99% (MeOH:H₂O = 50:50, 0.8 mL/min, $t_R = 4.35$ min).

4.1.8.15. N-Cyclohexyl-6-methoxy-3-(4-(3,4,5-trimethoxyphenyl)-1H-1,2,3-triazol-1-yl)benzofuran-2-carboxamide (17f). Yield: 67%; yellow solid; m.p.: 177–179 °C; ^1H NMR (600 MHz, CDCl_3) δ 9.33 (s, 1H), 8.21 (d, $J = 9.0$ Hz, 1H), 7.20 (s, 2H), 7.05 (dd, $J = 7.2, 1.8$ Hz, 1H), 7.03 (d, $J = 1.8$ Hz, 1H), 6.72 (d, $J = 8.4$ Hz, 1H), 4.02–3.98 (m, 1H), 3.97 (s, 6H), 3.91 (s, 3H), 3.90 (s, 3H), 2.06 (dd, $J = 9.0, 3.0$ Hz, 2H), 1.80 (td, $J = 6.6, 3.6$ Hz, 2H), 1.68 (dd, $J = 6.0, 3.6$ Hz, 1H), 1.49–1.42 (m, 2H), 1.38–1.31 (m, 2H), 1.27–1.25 (m, 1H); ^{13}C NMR (150 MHz, CDCl_3) δ 161.2, 157.4, 153.8, 153.7, 146.8, 138.6, 135.0, 126.0, 124.8, 123.5, 123.0, 116.3, 114.6, 103.6 (2C), 95.4 (2C), 61.0, 56.4 (2C), 55.8, 48.5, 33.2 (2C), 25.5, 24.9 (2C); MS (ESI) m/z 507.2 for $[\text{M}+1]^+$; HRMS (ESI) 507.2253 for $[\text{M}+\text{H}]^+$ (calcd 507.2238 for $\text{C}_{27}\text{H}_{31}\text{N}_4\text{O}_6$); HPLC purity > 99% (MeOH:H₂O = 50:50, 0.8 mL/min, $t_R = 4.20$ min).

4.1.8.16. 6-Methoxy-N-phenyl-3-(4-(3,4,5-trimethoxyphenyl)-1H-1,2,3-triazol-1-yl)benzofuran-2-carboxamide (17g). Yield: 58%; yellow solid; m.p.: 184–176 °C; ^1H NMR (600 MHz, CDCl_3) δ 9.19 (s, 1H), 8.68 (s, 1H), 8.15 (d, $J = 8.4$ Hz, 1H), 7.61–7.59 (m, 2H), 7.51–7.49 (m, 2H), 7.18 (s, 2H), 7.04 (d, $J = 8.4$ Hz, 1H), 7.00 (s, 1H), 3.96 (s, 6H), 3.90 (s, 3H), 3.89 (s, 3H); ^{13}C NMR (150 MHz, CDCl_3) δ 161.6, 156.1, 154.0, 153.7, 146.9, 138.6, 136.9, 134.5, 129.2 (2C), 125.7, 125.2, 124.7, 124.3, 122.8, 120.5 (2C), 116.1, 114.9, 103.6 (2C), 95.4 (2C), 60.9, 56.4, 55.8; MS (ESI) m/z 501.2 for $[\text{M}+1]^+$; HRMS (ESI) 501.1781 for $[\text{M}+\text{H}]^+$ (calcd 501.1769 for $\text{C}_{27}\text{H}_{25}\text{N}_4\text{O}_6$); HPLC purity > 99% (MeOH:H₂O = 60:40, 0.8 mL/min, $t_R = 4.28$ min).

4.1.8.17. (6-Methoxy-3-(4-(3,4,5-trimethoxyphenyl)-1H-1,2,3-triazol-1-yl)benzofuran-2-yl)(piperidin-1-yl)methanone (17h). Yield: 62%; yellow solid; m.p.: 179–181 °C; ^1H NMR (400 MHz, CDCl_3) δ 8.66 (d, $J = 4.0$ Hz, 1H), 7.90 (q, $J = 4.0$ Hz, 1H), 7.10 (s, 2H), 7.00–6.97 (m, 2H), 3.90 (s, 6H), 3.85 (s, 3H), 3.83 (s, 3H), 3.65 (s, 2H), 3.39 (s, 2H), 1.62 (s, 6H); ^{13}C NMR (150 MHz, CDCl_3) δ 160.5, 159.0, 154.1, 153.8 (2C), 147.3, 138.6, 137.9, 125.8, 122.7, 121.6, 115.8, 114.4, 103.4 (2C), 95.8, 61.0, 56.4 (2C), 55.8, 48.2, 43.8, 26.5, 25.6, 24.4 (2C); MS (ESI) m/z 493.2 for $[\text{M}+1]^+$; HRMS (ESI) 493.2093 for $[\text{M}+\text{H}]^+$ (calcd 493.2082 for $\text{C}_{26}\text{H}_{29}\text{N}_4\text{O}_6$); HPLC purity > 99%

(MeOH:H₂O = 60:40, 0.8 mL/min, *t_R* = 4.22 min).

4.1.8.18. (6-Methoxy-3-(4-(3,4,5-trimethoxyphenyl)-1H-1,2,3-triazol-1-yl)benzofuran-2-yl)(piperidin-1-yl)methanone (**17i**). Yield: 57%; yellow solid; m.p.: 183–185 °C; ¹H NMR (400 MHz, CDCl₃) δ 8.71 (s, 1H), 7.90 (q, *J* = 4.0 Hz, 1H), 7.11 (s, 2H), 7.03–6.95 (m, 2H), 3.90 (s, 6H), 3.85 (s, 3H), 3.83 (s, 3H), 3.75–3.55 (m, 8H); ¹³C NMR (150 MHz, CDCl₃) δ 160.9, 159.1, 154.1, 153.8 (2C), 147.3, 138.6, 136.8, 125.7, 122.9, 122.0, 115.7, 114.7, 103.5 (2C), 95.7 (2C), 66.8 (2C), 61.0, 56.4 (2C), 55.9, 47.5, 43.1; MS (ESI) *m/z* 495.2 for [M+1]⁺; HRMS (ESI) 495.1888 for [M+H]⁺ (calcd 495.1874 for C₂₅H₂₇N₄O₇); HPLC purity 96.1% (MeOH:H₂O = 30:70, 0.8 mL/min, *t_R* = 4.08 min).

4.2. Biology

4.2.1. Antiproliferation assays

Cells grown in the logarithmic phase were seeded into 96-well plates (5 × 10³ cells/well) for 24 h, and then exposed to different concentrations of the test compounds for 72 h. After attached cells were incubated with 5 mg/mL MTT (Sigma, USA) for another 4 h, the suspension was discarded, and subsequently the dark blue crystals (formazan) were solubilized in dimethyl sulfoxide (DMSO). The absorbance of the solution at 490 nm was measured using a multifunction microplate reader (Molecular Devices, Flex Station 3), and each experiment was performed at least in triplicate. IC₅₀ values, which represent the drug concentrations required to cause 50% cancer cell growth inhibition, were used to express the cytotoxic effects of each compound and were calculated with GraphPad Prism Software version 5.02 (GraphPad Inc., La Jolla, CA, USA).

4.2.2. In vitro tubulin polymerization assay

Pig brain microtubule protein was isolated by three cycles of temperature-dependent assembly/disassembly according to Shelanski et al in 100 mM PIPES (pH 6.5), 1 mM MgSO₄, 2 mM EGTA, 1 mM GTP and 1 mM 2-mercaptoethanol. In the first cycle of polymerization, glycerol and phenylmethylsulfonyl fluoride were added to 4 M and 0.2 mM, respectively. Homogeneous tubulin was prepared from microtubule protein by phosphocellulose (P11) chromatography. The purified proteins were stored in aliquots at -70 °C. Tubulin protein was mixed with different concentrations of compound in PEM buffer (100 mM PIPES, 1 mM MgCl₂, and 1 mM EGTA) containing 1 mM GTP and 5% glycerol. Microtubule polymerization was monitored at 37 °C by light scattering at 340 nm using a SPECTRA MAX 190 (Molecular Device) spectrophotometer. The plateau absorbance values were used for calculations.

4.2.3. Immunofluorescence microscopy

In a 10 mm confocal culture dish, 3 × 10⁴ cells were grown for 24 h and then incubated in the presence or absence of compound **17g** at the indicated concentrations for another 6 h. After being washed with phosphate-buffered solution (PBS) and fixed in 4% prewarmed (37 °C) paraformaldehyde for 15 min, the cells were permeabilized with 0.5% Triton X-100 for 15 min and blocked for 30 min in 10% goat serum. Then, the cells were incubated with mouse anti-tubulin antibody (CST, USA) at 4 °C overnight, washed with PBS three times, and incubated with goat antimouse IgG/Alexa-Fluor 488 antibody (Invitrogen, USA) for 1 h. The samples were immediately visualized on a Zeiss LSM 570 laser scanning confocal microscope (Carl Zeiss, Germany) after the nuclei were stained with DAPI (Solarbio, Chin) in the dark at room temperature for 10 min.

4.2.4. Cell cycle analysis

A549 cells were seeded in 6-well plates (3 × 10⁵ cells/well), incubated in the presence or absence of compound **17g** at the indicated concentrations for 24 h, harvested by centrifugation, and then fixed in ice-cold 70% ethanol overnight. After the ethanol was removed the next day, the cells were resuspended in ice-cold PBS, treated with RNase A

(Keygen Biotech, China) at 37 °C for 30 min, and then incubated with the DNA staining solution propidium iodide (PI, Keygen Biotech, China) at 4 °C for 30 min. Approximately 10 000 events were detected by flow cytometry (Beckman Coulter, Epics XL) at 488 nm.

4.2.5. Western blot analysis

A549 cells (5.0 × 10⁵ cells/dish) were incubated with or without **17g** at various concentrations for 6 h. After incubation, the cells were collected by centrifugation and washed twice with phosphate-buffered saline chilled to 0 °C. Then, the cells were homogenized in RIPA lysis buffer containing 150 mM NaCl, 50 mM Tris (pH 7.4), 1% (w/v) sodium deoxycholate, 1% (v/v) Triton X-100, 0.1% (w/v) SDS, and 1 mM EDTA (Beyotime, China). The lysates were incubated on ice for 30 min, intermittently vortexed every 5 min, and centrifuged at 12 500 g for 15 min to harvest the supernatants. Next, the protein concentrations were determined by a BCA Protein Assay Kit (Thermo Fisher Scientific, Rockford, Illinois, USA). The protein extracts were reconstituted in loading buffer containing 62 mM Tris - HCl, 2% SDS, 10% glycerol, and 5% β-mercaptoethanol (Beyotime, China), and the mixture was boiled at 100 °C for 10 min. An equal amount of the proteins (50 mg) was separated by 8–12% sodium dodecyl sulfate–polyacrylamide gel electrophoresis (SDS-PAGE) and transferred to nitrocellulose membranes (Amersham Biosciences, Little Chalfont, Buckinghamshire, UK). Then, the membranes were blocked with 5% nonfat dried milk in TBS containing 1% Tween-20 for 90 min at room temperature and were incubated overnight with specific primary antibodies (CST, USA) at 4 °C. After three washes in TBST, the membranes were incubated with the appropriate HRP-conjugated secondary antibodies at room temperature for 2 h. The blots were developed with enhanced chemiluminescence (Pierce, Rockford, Illinois, USA) and were detected by an LAS4000 imager (GE Healthcare, Waukesha, Wisconsin, USA).

4.2.6. Apoptosis analysis

A549 cells were seeded in 6-well plates (3 × 10⁵ cells/well), incubated in the presence or absence of compound **17g** at the indicated concentrations for 12 h. After incubation, cells were harvested and incubated with 5 μL of Annexin-V/FITC (Keygen Biotech, China) in binding buffer (10 mM HEPES, 140 mM NaCl, and 2.5 mM CaCl₂ at pH 7.4) at room temperature for 15 min. PI solution was then added to the medium for another 10 min incubation. Almost 10 000 events were collected for each sample and analyzed by flow cytometry (Beckman Coulter, Epics XL).

4.2.7. Mitochondrial membrane potential assay

A lipophilic cationic dye, 5,5',6,6'-tetrachloro-1,1',3,3'-tetraethylbenzimidazolcarbocyanine (JC-1, Beyotime, China), was used to monitor the level of MMP in the cells. At normal state, the MMP is high and JC-1 appears as aggregates, indicated by red fluorescence. When apoptosis occurs, the MMP is reduced and JC-1 appears as monomers, indicated by green fluorescence. Two methods including flow cytometry and fluorescence microscopy were used to detect the MMP. For the fluorescence microscopy detection, A549 cells were plated in 6-well plates (3 × 10⁵ cells/well), incubated for 24 h, and treated with **17g** at the indicated concentrations for another 6 h. Then, the cells were stained with 2 μM JC-1 at 37 °C for 30 min and washed with PBS, and then the cell nuclei were stained with DAPI (Solarbio, China) for 10 min in the dark. The cell images were immediately visualized on a Zeiss LSM 570 laser scanning confocal microscope (Carl Zeiss, Germany).

4.2.8. Molecular docking

In this study, the tubulin structure was downloaded from the Protein Data Bank (PDB code 1SA0). Using Schrodinger software to prepare the protein by removing of Mg²⁺, water molecules and colchicine. Then the ligand **17g** was minimized. The docking procedure was performed by employing docking program in schrodinger software, and the structural image was obtained using PyMOL software.

Acknowledgements

This work was financially supported by the National Natural Sciences Foundations of China (21672093).

Declaration of Competing Interest

The authors declare that they have no competing interests.

Appendix A. Supplementary material

Supplementary data to this article can be found online at <https://doi.org/10.1016/j.bioorg.2019.103392>.

References

- [1] K.H. Downing, E. Nogales, Tubulin and microtubule structure, *Curr. Opin. Cell Biol.* 10 (1998) 16–22.
- [2] M.A. Jordan, L. Wilson, Microtubules as a target for anti-cancer drugs, *Nat. Rev. Cancer.* 4 (2004) 253–265.
- [3] P. Ea, Microtubule inhibitors: Differentiating tubulin-inhibiting agents based on mechanisms of action, clinical activity, and resistance, *Mol. Cancer Ther.* 8 (2009) 2086–2095.
- [4] D. Charles, J. Mary Ann, Microtubule-binding agents: a dynamic field of cancer therapeutics, *Nat. Rev. Drug Discov.* 9 (2010) 790–803.
- [5] Y. Lu, J. Chen, M. Xiao, W. Li, D.D. Miller, An overview of tubulin inhibitors that interact with the colchicine binding site, *Pharm. Res.* 29 (2012) 2943–2971.
- [6] T. Fojo, M. Meneffee, Mechanisms of multidrug resistance: the potential role of microtubule-stabilizing agents, *Ann. Oncol.* 18 (S5) (2007) v3–v8.
- [7] P.D.W. Eckford, F.J. Sharom, ABC efflux pump-based resistance to chemotherapy drugs, *Chem. Rev.* 109 (2009) 2989–3011.
- [8] E. Boyland, M.E. Boyland, Studies in tissue metabolism, *Biochem. J.* 31 (1937) 454–460.
- [9] W. Li, H. Sun, S. Xu, Z. Zhu, J. Xu, Tubulin inhibitors targeting the colchicine binding site: a perspective of privileged structures, *Future Med. Chem.* 9 (2017) 1765–1794.
- [10] G.C. Tron, T. Piralì, G. Sorba, F. Pagliari, S. Busacca, A.A. Genazzani, Medicinal chemistry of combretastatin A4: present and future directions, *J. Med. Chem.* 49 (2006) 3033–3044.
- [11] (a) G. Shreeves, L. Poupard, M. Zweifel, G.J.S. Rustin, G.C. Jayson, N.S. Reed, R. Osborne, B. Hassan, J. Ledermann, D.J. Chaplin, J. Balkissoon, S.-P. Lu, Phase II trial of combretastatin A4 phosphate, carboplatin, and paclitaxel in patients with platinum-resistant ovarian cancer, *Ann. Oncol.* 22 (2011) 2036–2041; (b) Mateon therapeutics announces termination of FOCUS study in ovarian cancer and restructuring to prioritize OXi4503 for AML. <http://investor.mateon.com/news-releases/news-release-details/mateon-therapeutics-announces-termination-focus-study-ovarian?ReleaseID=1041745>.
- [12] C. Anurag, S.N. Pandeya, P. Kumar, P.P. Sharma, S. Gupta, N. Soni, K.K. Verma, G. Bhardwaj, Combretastatin A-4 analogs as anticancer agents, *Mini-Rev. Med. Chem.* 7 (2007) 1186–1205.
- [13] K. Donthiboina, P. Anchi, P.V. Sri Ramya, S. Karri, G. Srinivasulu, C. Godugu, N. Shankaraiah, A. Kamal, Synthesis of substituted biphenyl methylene indolinones as apoptosis inducers and tubulin polymerization inhibitors, *Bioorg. Chem.* 86 (2019) 210–223.
- [14] Q. Lai, Y. Wang, R. Wang, W. Lai, L. Tang, Y. Tao, Y. Liu, R. Zhang, L. Huang, H. Xiang, S. Zeng, L. Gou, H. Chen, Y. Yao, J. Yang, Design, synthesis and biological evaluation of a novel tubulin inhibitor **7a3** targeting the colchicine binding site, *Eur. J. Med. Chem.* 156 (2018) 162–179.
- [15] M. Mustafa, D. Abdelhamid, E.M.N. Abdelhafez, M.A.A. Ibrahim, A.M. Gamal-Eldeen, O.M. Aly, Synthesis, antiproliferative, anti-tubulin activity, and docking study of new 1,2,4-triazoles as potential combretastatin analogues, *Eur. J. Med. Chem.* 141 (2017) 293–305.
- [16] T. Naret, J. Bignon, G. Bernadat, M. Benckroun, H. Levaïque, C. Lenoir, J. Dubois, A. Pruvost, F. Saller, D. Borgel, B. Manoury, V. Leblais, R. Darrigrand, S. Apcher, J.-D. Brion, E. Schmitt, F.R. Leroux, M. Alami, A. Hamze, A fluorine scan of a tubulin polymerization inhibitor isocombretastatin A-4: design, synthesis, molecular modelling, and biological evaluation, *Eur. J. Med. Chem.* 143 (2018) 473–490.
- [17] R. Romagnoli, P.G. Baraldi, M.K. Salvador, F. Prencipe, C. Lopez-Cara, S. Schiaffino Ortega, A. Brancale, E. Hamel, I. Castagliuolo, S. Mitola, R. Ronca, R. Bortolozzi, E. Porcu, G. Basso, G. Viola, Design, synthesis, in vitro, and in vivo anticancer and antiangiogenic activity of novel 3-arylamino-benzofuran derivatives targeting the colchicine site on tubulin, *J. Med. Chem.* 58 (2015) 3209–3222.
- [18] G. La Regina, R. Bai, A. Coluccia, V. Famigliani, S. Pelliccia, S. Passacantilli, C. Mazzoccoli, V. Ruggieri, A. Verrico, A. Miele, L. Monti, M. Nalli, R. Alfonsi, L. Di Marcotullio, A. Gulino, B. Ricci, A. Soriani, A. Santoni, M. Caraglia, S. Porto, E. Da Pozzo, C. Martini, A. Brancale, L. Marinelli, E. Novellino, S. Vultaggio, M. Varasi, C. Mercurio, C. Bigogno, G. Dondio, E. Hamel, P. Lavia, R. Silvestri, New indole tubulin assembly inhibitors cause stable arrest of mitotic progression, enhanced stimulation of natural killer cell cytotoxic activity, and repression of hedgehog-dependent cancer, *J. Med. Chem.* 58 (2015) 5789–5807.
- [19] B.L. Flynn, G.S. Gill, D.W. Grobelny, J.H. Chaplin, D. Paul, A.F. Leske, T.C. Lavranos, D.K. Chalmers, S.A. Charman, E. Kostewicz, D.M. Shackelford, J. Morizzi, E. Hamel, M.K. Jung, G. Kremmidiotis, Discovery of 7-hydroxy-6-methoxy-2-methyl-3-(3,4,5-trimethoxybenzoyl)benzo[b]furan (BNC105), a tubulin polymerization inhibitor with potent antiproliferative and tumor vascular disrupting properties, *J. Med. Chem.* 54 (2011) 6014–6027.
- [20] G. Kremmidiotis, A. Leske, J. Simpson, E. Doolin, J. Iglesias, Identification of plasma biomarker concentration changes resulting from the administration of the vascular disrupting agent BNC105 across 3 clinical trials in mesothelioma, ovarian and renal cancer, *Cancer Res.* 75 (2015) 1186–1205.
- [21] (a) K. Odlo, J. Fournier-Dit-Chabert, S. Ducki, O.A. Gani, I. Sylte, T.V. Hansen, 1,2,3-triazole analogs of combretastatin A-4 as potential microtubule-binding agents, *Bioorg. Med. Chem.* 18 (2010) 6874–6885; (b) Ø.W. Akselsen, K. Odlo, J.-J. Cheng, G. Maccari, M. Botta, T.V. Hansen, Synthesis, biological evaluation and molecular modeling of 1,2,3-triazole analogs of combretastatin A-1, *Bioorg. Med. Chem.* 20 (2012) 234–242.
- [22] R. Kharb, P.C. Sharma, M.S. Yar, Pharmacological significance of triazole scaffold, *J. Enzym. Inhib. Med. Chem.* 26 (2011) 1–21.
- [23] J.-L. Mi, C.-H. Zhou, X. Bai, Advances in triazole antimicrobial agents, *Chin. J. Antibio.* 32 (2007) 587–593.
- [24] H. Konno, T. Sato, Y. Saito, I. Sakamoto, K. Akaji, Synthesis and evaluation of aminopyridine derivatives as potential BACE1 inhibitors, *Bioorg. Med. Chem. Lett.* 25 (2015) 5127–5132.
- [25] M.M. Heravi, S. Asadi, N. Nazari, B. Malekzadeh Lashkariani, Developments of Corey-Fuchs Reaction in organic and total synthesis of natural products, *Curr. Org. Chem.* 19 (2015) 2196–2219.
- [26] M.I. Mangione, R.A. Spanevello, M.B. Anzardi, Efficient and straightforward click synthesis of structurally related dendritic triazoles, *RSC Adv.* 7 (2017) 47681–47688.
- [27] G. Krishnaswamy, N.R. Desai, K. Potla, D.S. P. A, A.K. Basappa, Synthesis, characterization, crystal structure and DFT calculations of 1-benzofuran-2-carboxylic acid, *Der Pharma Chemica.* 8 (2016) 46–54.
- [28] Z.-B. Tang, Y.-Z. Chen, J. Zhao, X.-W. Guan, Y.-X. Bo, S.-W. Chen, L. Hui, Conjugates of podophyllotoxin and norcantharidin as dual inhibitors of topoisomerase II and protein phosphatase 2A, *Eur. J. Med. Chem.* 123 (2016) 568–576.
- [29] J.-F. Liu, C.-Y. Sang, X.-H. Xu, L.-L. Zhang, L. Hui, J.-B. Zhang, S.-W. Chen, Synthesis and cytotoxic activity on human cancer cells of carbamate derivatives of 4β-(1,2,3-triazol-1-yl)podophyllotoxin, *Eur. J. Med. Chem.* 64 (2013) 621–628.
- [30] C.-Y. Sang, W.-W. Qin, X.-J. Zhang, Y. Xu, Y.-Z. Ma, X.-R. Wang, L. Hui, S.-W. Chen, Synthesis and identification of 2,4-bis(aminopyrimidines) bearing 2,2,6,6-tetramethylpiperidine-N-oxyl as potential Aurora A inhibitors, *Bioorg. Med. Chem.* 27 (2019) 65–78.
- [31] M.L. Shelanski, F. Gaskin, C.R. Cantor, Microtubule assembly in the absence of added nucleotides, *NAS* 70 (1973) 765–768.
- [32] W. Li, Y. Yin, W. Shuai, F. Xu, H. Yao, J. Liu, K. Cheng, J. Xu, Z. Zhu, S. Xu, Discovery of novel quinazolines as potential anti-tubulin agents occupying three zones of colchicine domain, *Bioorg. Chem.* 83 (2019) 380–390.
- [33] C. Dominguez-Brauer, K. Thu, J. Mason, H. Blaser, M. Bray, T. Mak, Targeting mitosis in cancer: Emerging Strategies, *Mol. Cell* 60 (2015) 524–536.
- [34] A. Ca, B. Jc, Cell cycle controls: potential targets for chemical carcinogens, *Environ. Health Perspect.* 101 (1993) 9–14.
- [35] M. Jackman, C. Lindon, E.A. Nigg, J. Pines, Active cyclin B1-Cdk1 first appears on centrosomes in prophase, *Nat. Cell Biol.* 5 (2003) 143–148.
- [36] R. Romeo, B. Pier Giovanni, S. Maria Kimatrai, P. Filippo, L.C. Carlota, S.O. Santiago, B. Andrea, H. Ernest, C. Ignazio, M. Stefania, Design, synthesis, in vitro, and in vivo anticancer and antiangiogenic activity of novel 3-arylamino-benzofuran derivatives targeting the colchicine site on tubulin, *J. Med. Chem.* 58 (2015) 3209–3222.
- [37] W. Li, W. Shuai, H. Sun, F. Xu, Y. Bi, J. Xu, C. Ma, H. Yao, Z. Zhu, S. Xu, Design, synthesis and biological evaluation of quinoline-indole derivatives as anti-tubulin agents targeting the colchicine binding site, *Eur. J. Med. Chem.* 163 (2019) 428–442.
- [38] M.C. Wei, W.X. Zong, E.H. Cheng, T. Lindsten, V. Panoutsakopoulou, A.J. Ross, K.A. Roth, G.R. Macgregor, C.B. Thompson, S.J. Korsmeyer, Proapoptotic BAX and BAK: a requisite gateway to mitochondrial dysfunction and death, *Science.* 292 (2001) 727–730.
- [39] Krishnendu Sinha, P. Joydeep, C. Parames Bikash, Oxidative stress: the mitochondria-dependent and mitochondria-independent pathways of apoptosis, *Arch. Toxicol.* 87 (2013) 1157–1180.
- [40] R.B.G. Ravelli, B. Gigant, P.A. Curmi, I. Jourdain, S. Lachkar, A. Sobel, M. Knossow, Insight into tubulin regulation from a complex with colchicine and a stathmin-like domain, *Nature* 428 (2004) 198–202.